KWAME NKRUMAH UNIVERSITY OF SCIENCE AND TECHNOLOGY

COLLEGE OF ENGINEERING

DEPARTMENT OF GEOMATIC ENGINEERING

ANALYSIS OF SURFACE INTERPOLATION ALGORITHMS FOR DIFFERENT SURFACE TYPES

A THESIS SUBMITTED TO THE DEPARTMENT OF GEOMATIC ENGINEERING, KWAME NKRUMAH UNIVERSITY OF SCIENCE AND TECHNOLOGY IN PARTIAL FULFILMENT OF THE REQUIREMENTS FOR THE DEGREE OF MASTER OF SCIENCE IN GEOMATIC ENGINEERING

BY

SAFO KOFI AGYEI

SUPERVISORS

PROF. ERIC K. FORKUO

REV. JOHN AYER

OCTOBER, 2016

DECLARATION

I hereby declare that this submission is my own work towards the MSc and that, to the best of my knowledge, it contains no material previously published by another person, nor material which has been accepted for the award of any other degree of the University except where due acknowledgement has been made in the text.

SAFO KOFI AGYEI (PG2233314) ……………………………… ……………………..
Student & ID Signature Date

PROF. ERIC K. FORKUO ……………………………… ……………………..
(Supervisor) Signature Date

Certified by:

REV. JOHN AYER ……………………………… ……………………..
(Supervisor) Signature Date

Certified by:

Dr. Isaac Dadzie ……………………………… ……………………..
(Head of Department) Signature Date

ABSTRACT

Digital Terrain Models (DTMs) has become a very significant tool in extracting geomorphological information from various land areas. Their use is in the fields of mapping, landscape planning, urban design and many more. Automatic stereocorrelation has been used to generate a DTM from ASTER stereo image pair (3N and 3B) using ENVI software. Elevation values were extracted and used with four different interpolation algorithms. The resulting surfaces when compared with those from the topographic map showed that the Inverse Distance Weighting (IDW) can achieve a Root Mean Square Error (RMSE) of ±10.773m and Mean Absolute Error (MAE) of ±8.714m for flat terrain as compared to RMSE of ±11.035m, MAE of ±8.999m for spline; RMSE of ±11.121m, MAE of ±9.102m for Natural Neighbour (NN) and RMSE of ±12.108m, MAE of ±9.979m for kriging interpolation method using a point density of 61.49 points per km^2. Hence, IDW is best for this surface type. For undulating terrain, IDW again gave the least RMSE of ±13.549m and MAE of ±10.789m in comparison to RMSE of ±13.711m, MAE of ±10.963m for NN; RMSE of ±13.717m, MAE of ±11.028m for spline and RMSE of ±14.835m, MAE of ±11.658m for kriging interpolation method for point density 62.30 points per km^2 and hence, IDW is again best for this surface type. For mountainous terrain, NN interpolation method with RMSE of ±19.044m and MAE of ±13.909m gave best results than the other interpolation types. RMSE of ±21.167m, MAE of ±15.241m was obtained for kriging; RMSE of ±21.632, MAE of ±14.687m for IDW and RMSE of ±21.721m, MAE of ±14.544m for spline for point density 141.64 points per km^2 and so NN works best for mountainous terrains. It is therefore recommended that IDW interpolation algorithm should be used for both flat and undulating terrains whereas NN should also be used for mountainous terrains.

ABBREVIATIONS / ACRONYMS

ASTER	-	Advanced Spaceborne Emmission and Reflection Radiometer
AVG	-	Average
DEM	-	Digital Elevation Model
DSM	-	Digital Surface Model
DTM	-	Digital Terrain Model
GCP	-	Ground Control Point
GIS	-	Geographic Information System
HDF	-	Hieratical Data Format
IDW	-	Inverse Distance Weighting
ICP	-	Independent Check Points
KNUST	-	Kwame Nkrumah University of Science and Technology
MAE	-	Mean Absolute Error
NN	-	Natural Neighbour
RMSE	-	Root Mean Squared Error
RPC	-	Rational Polynomial Coefficients
TIN	-	Triangulated Irregular Network
UTM	-	Universal Transverse Mercator
ΔZ	-	Difference between the elevations of the ASTER-DTM and the check points

TABLE OF CONTENTS

LIST OF TABLES

LIST OF FIGURES

ACKNOWLEDGMENT

I wish to express my profound gratitude to the Lord Almighty, whose divine favour, strength and wisdom has led me to complete this study.

My immeasurable gratitude also goes to the staff of Geomatic Engineering Department, KNUST, especially my supervisors Rev. John Ayer and Prof. E. K. Forkuo for their dedicated direction, guidance and various ways by which they assisted me in completing this work.

Finally, I wish to express my sincerest appreciation to my friends and family especially my parents Mr. Daniel Safo and Mrs. Cecilia Osei for their unconditional love, care and support that led to the successful completion of this work.

CHAPTER ONE

INTRODUCTION

1.1 Background of Study

Land surfaces are generally represented in a computer environment as DTMs (Weibel and Heller, 1999). These digital representations are modeled from terrain reliefs through collections of data samples and algorithms which can interpolate elevations of intermediate unknown points. DTMs have several possible applications such as in the field of military where usage ranges from surveillance and intelligence gathering to strategic planning in battle field as a guide in missile launching. DTMs also play an integrate part in creating relief maps. Accurate elevation data helps geologists to determine and extract various geomorphological information from various terrain characteristics.

Advancement in technology has increased extensively the capability of DTMs generation from satellite images to more accurately represent terrains, making it useful in the field of civil engineering, landscape planning, urban design and road traffic engineering. Integration of DTM data with Geographic Information System (GIS) provides opportunity to model terrain relief, analyze and visualize phenomenon related to topography.

Over the year's digital representation of terrains have been denoted severally as DTM, Digital Elevation Model (DEM) or Digital Surface Model (DSM). Although these terms are mostly used synonymously, the difference or meaning basically lies in its mode of application (Oksanen, 2006). DSM data includes low rise and high rise buildings, roads, bridges, forest trees and structures that can be found on the surface of the earth (Maune *et al*. 2007). DEM data does not necessarily include objects or manmade features on the surface of the earth, but mostly represents the bare ground with natural phenomenon like rivers (Oksanen, 2006;

Maune *et al*. 2007). A DTM on the other hand is a continuous or smooth surface which aside from the values of elevations grids, also consists of other elements that describe the topographic surface such as slope, aspect, curvature, gradient, skeleton (pits, saddles, ridges, peaks) and others (Podobnikar, 2005). The DEM is often used generically for DTM (Maune *et al*. 2007; Li *et al*, 2005).

DTMs can be represented and stored in several ways. The commonly used data formats for DTMs are, (i) the regular grid (raster) and (ii) the Triangulated Irregular Network (TIN) (Weibel and Heller, 1991; Peng *et al*, 2004). The TIN transforms an irregularly spaced points data thus (x, y, z) values to form contiguous, non-overlapping, triangles that represents the surface. The TIN model allows extra data in complex areas and less data in non-complex areas thereby reducing redundancy. This therefore enables it to represent information about altitude, slope and aspects. However, they can be quite demanding towards memory space and computing time and also the algorithms involved could be sophisticated (De Wulf *et al*, 2012).

DTMs grid according to Weibel and Heller (1991) gives a matrix structure that records topological relation between data points stored as a two-dimensional array of elevations. Although the raster format has a number of setbacks which involves a rectangular data array irrespective of the morphology of the terrain, it remains the most popular format in the foreseeable future (Pike *et al*, 2009). This is because, it represents a terrain in a more technically controlled manner of grid cells where each cell could have its own property (Hengl, 2006). Grid DTMs ensures simplicity of the models and low memory space requirements whilst allowing for fast and straightforward data computations (De Wulf *et al*, 2012).

In DTMs elevations are presented as surface values on the land surface in areas of interest.

Shi *et al* (2005) recognized that the overall accuracy of a generated DTM depends on both the propagation error and the model error. Leberl (1973) also asserted that a DTM performance depend on the terrain and the method used in interpolating the new points from the existing measurements. This therefore suggests that, apart from a good sampling of points required to improve the quality of any DTM, a good modelling of the surface would also depend on the appropriate DTM interpolation method chosen and used.

Many research works have been conducted on the various interpolation algorithms, however, an understanding of the terrain conditions upon which the interpolation is performed have largely been ignored. Hengl *et al* (2009) therefore claimed that, an inexperienced user would mostly be confused as to which technique to select in order to produce a DTM that would best suit a particular purpose. There are various data sources for DTMs. These data sources are severally aerial photography, satellite imagery, cartographic maps and measured terrestrial points.

1.2 Problem Statement

Many techniques exist for interpolating to approximate a surface from elevation data exists. The accuracy of the resulting surfaces depends on the nature of the landform and the interpolating algorithm used for interpolating the surface. There is no technique defined for different landforms but the user has to experiment with different techniques to select the best that will fit each landform type or just use any randomly irrespective of whether it is the best for the circumstance or not. The implementation and determination of which interpolation type is best for each landform type poses a problem which is the objective of this research

1.3 Aim and Objectives

1.3.1 Aim

The aim of this thesis is to implement various interpolation algorithms on different terrain types and determine which algorithm is most suitable for which type of terrain.

1.3.2 Specific Objectives

The objectives of the research are;

1. To generate DTMs from ASTER stereo imagery.
2. To investigate how the various interpolation algorithms perform with different terrain characteristics.
3. To determine the quality of DTM generated.

1.4 Research Questions

1. How many interpolation points are needed for DTM generation for each interpolation type?
2. What interpolating algorithm is best suited for the different terrains?
3. What is the quality of the generated surface?

1.5 Organization of Thesis

The work represented here are structured into five chapters.

Chapter 1 is an introductory chapter that includes a background to the study and problem statement. The main aim and objectives are also laid out here. A number of research questions are posed to answer the objectives.

In chapter 2, DTM generation and interpolation methods are discussed. This chapter contains literature about DTM sources and the generation of DTM from ASTER. Interpolation types and methods, as well as the errors associated with interpolation and previous work that have been done are also reviewed.

The materials and the methodology applied in the current study are discussed in chapter 3. This include the processes involved in DTM generation, issue of contour derived DTM, DTM modelling, study area and dataset preparation for interpolation.

The results obtained are stated in chapter 4. This chapter also contains a discussion of the results.

The main findings are stated in chapter 5 as conclusions. Some recommendations are also made towards further research in this chapter

CHAPTER TWO

DTM GENERATION AND INTERPOLATION METHODS

2.1 Data Sources for Digital Terrain Modelling

Nelson *et al* (2009) and Deilami *et al* (2012) identified three main sources of deriving DTMs as: (i) Ground surveys - which is the most accurate method of deriving both horizontal and vertical measurements (X, Y, Z). However, this method has quite a number of setbacks as the procedures adopted in the surveying could be tedious, time consuming, sometimes limited by access to some survey sites and also requiring highly experienced personnel's make the method expensive; (ii) From Topographic maps – where features of interests such as contours, elevations and rivers or streams are extracted and; (iii) Remote sensing – use different sensors. This is the fastest growing method of deriving DTM data as the numerous setbacks posed by the traditional methods are eliminated. The platform may either be airborne or spaceborne yielding images that include ASTER, RADAR, LIDAR and aerial photographs. Some of these platforms have sensors that are able to capture stereo pair images which contains accurate information about the elevation of the terrain. Examples of satellites offering the possibility for stereoscopic acquisition include: SPOT, MOMS, IRS,
KOMPSAT, AVNIR, TERRA, IKONOS, QUICKBIRD-2, SPOT-5, EROS-A1 and ORBVIEW-3 (Lee *et al*, 2008).

2.2 DTM Generation from ASTER

ASTER is an imaging instrument onboard the Terra platform, brought up by NASA, Japan's Ministry of Economy, Trade and Industry (METI) and Japan Space Systems as part of NASA's Earth Observing System (EOS) launched in December 1999. The main aim of the NASA Earth Observing System is to gain a better understanding of the earth and it has since become very useful in creating detailed maps of land surface temperature and elevations for various analysis.

ASTER stereo data is mostly used and appreciated because it is inexpensive and widely accessible, has global coverage and an along track capturing capability which enhances the accuracy of the image (Figure 2.1)

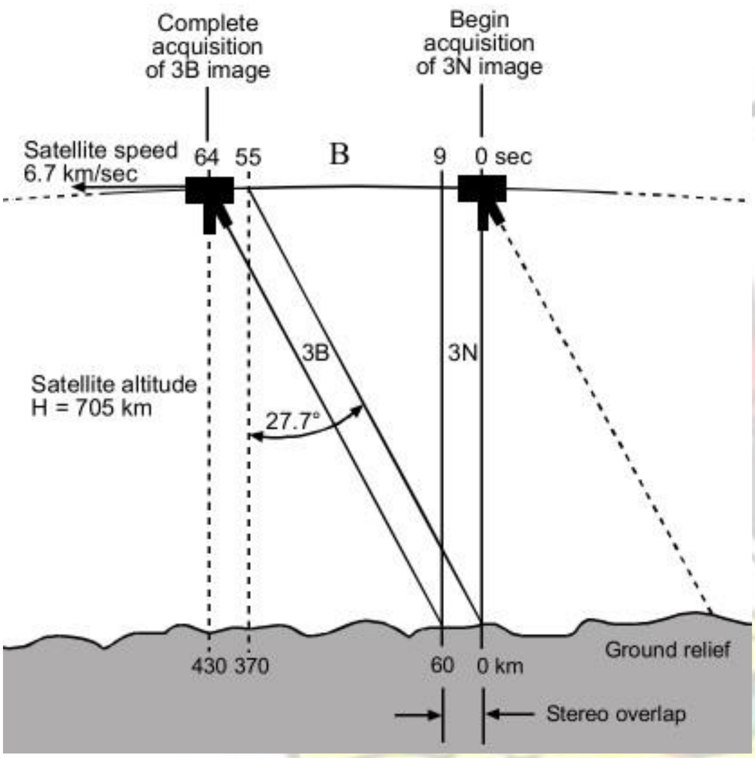

Figure 2.1: Image Geometry of ASTER Along-Track Stereo Pair (3N and 3B)

Source: http://asterweb.jpl.nasa.gov/

ASTER has a wide spectral region of 14 bands from visible to thermal infrared with high spatial, spectral and radiometric resolution. It possesses two very sensitive telescopes that provides an along track near infrared image which is stereoscopic in nature. One of the telescopes capture data in the nadir (N) direction whiles the other captures image data in the backward (B) direction thereby giving it an offsetting angle of 27.7 degrees when considering the earth as a curve (Fujisada *et al*. 2005). ASTER has a very good base-to-height ratio of

0.6, the duration of data capture between the nadir and the backward view is approximately 60 seconds and this enhances the accuracy of the image (ERSDAC, 2001).

The entire spectral region of the ASTER is covered by basically three band classes: (i) the Visible and Near Infrared Radiometer (VNIR) bands with a spatial resolution of 15m, (ii) six Short Wave Infrared Radiometer (SWIR) bands with a spatial resolution of 30m and (iii) five Thermal Infrared Radiometer (TIR) bands with a spatial resolution of 90m (Table 2.1). The terra satellite flies in a circular, near polar orbit at an altitude of 705 km. The orbit is sunsynchronous with equatorial crossing at local time of 10:30 a.m., returning to the same orbit every 16 days with swath width of 60 km (Toutin, 2008)

Table 2.1: General characteristics of the ASTER bands

Characteristics	VNIR	SWIR	TIR
Spectral Range	Band 1 0.52 - 060 µm Nadir looking	Band 4 1.600 - 1.700 µm	Band 10 8.125 - 8.475 µm
	Band 2 0.63 - 0.69 µm Nadir looking	Band 5 2.145 - 2.185 µm	Band 11 8.475 - 8.825 µm
	Band 3N 0.76 – 0.86 µm Nadir looking	Band 6 2.185 – 2.225 µm	Band 12 8.925 – 9.275 µm
	Band 3B 0.76 – 0.86 µm Backward looking	Band 7 2.235 – 2.285 µm	Band 13 10.25 – 10.95 µm
		Band 8 2.295 – 2.365 µm	Band 14 10.95 – 11.65 µm
		Band 9 2.360 – 2.430 µm	
Ground Resolution (m)	15	30	90
Data Rate (Mbits /sec)	62	23	4.2
Cross-track Pointing (deg.)	±24	±8.55	±8.55
Cross-track Pointing (km)	±318	±116	±116
Swath Width (km)	60	60	60
Quantization (bits)	8	8	12

Source: http://asterweb.jpl.nasa.gov/

2.2.1 Orientations of ASTER Stereo Pair Image

Absolute orientation of the sensors is mostly in reference to the mean sea level and with the presence of accurate Ground Control Point (GCP) say from topographic maps of known coordinates the 3N and 3B stereo pairs can be rectified (Hirano *et al*, 2003).

To be able to process the satellite image a suitable sensor model is required to define the geometric properties of the sensor. This depends on the positioning and orientation of the camera sensor in the object space. Orientation determines the procedure of transforming parameters from one coordinate to another. There are basically three forms of orientations and these are interior, relative and absolute orientations, necessary for the generation of DTM.

Interior Orientation

Interior orientation properties consist of the parameters that describes the internal geometry of the sensors as of when the images were captured. The primary focus is to transform the image pixel coordinate system to the image space coordinate system (Jain *et al*, 2008). With a proper rectification, possible errors associated with the digital image are minimized or removed. Figure 2 shows the internal geometry of the camera.

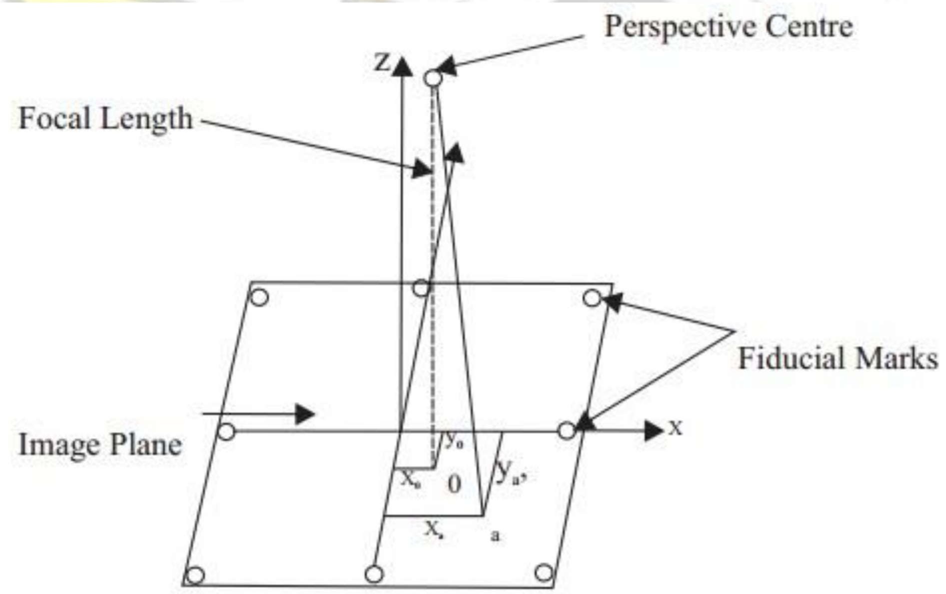

Figure 2.2: Internal Geometry

Source: ERDAS, 2003

Exterior Orientation

The essential role of providing exterior orientation parameters is to enhance the creation of orthorectified images. The Exterior orientation consists of the relative and absolute orientations and define both the original position and angular orientations with respect to the image (Jain, 2008; Ping, 2003). The relative orientation establishes a relationship between stereo pair images, achieved by describing the attitude and relative positions of the stereo pairs. Figure 2.3 shows the angular components Omega (Ω), Phi (φ) and Kappa (K) which describes the relationship between the ground space coordinate system (X, Y, Z) and the image space coordinates. The absolute orientation function to relate the image space to the object space, by the use of reliable and accurate GCP as parameters for coordinate transformation.

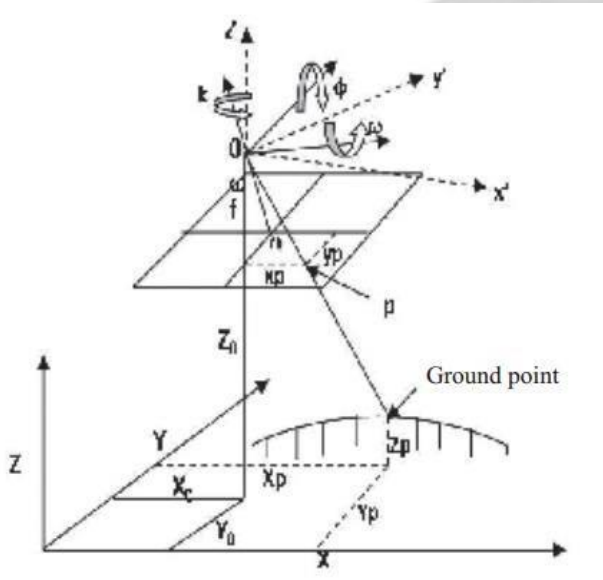

Figure 2.3: Components of Exterior Orientation

Source: ERDAS, 2003

2.2.2 Image Processing

Some of the off-the-shelf softwares used for processing ASTER stereo data and generating DTMs include: (Toutin, 2008, Deilami *et al*., 2012)

- Geomatica™ OrthoEngine® of PCI Geomatics;

- OrthoBase Pro™ module of ERDAS ImagineH and the LPS SP 2 of Leica Geosystems Geospatial Imaging;
- Desktop Mapping System (DMS)™ of R-WEL;
- SilcAst of Sensor Information Laboratory Corp.
- AsterDTM module.
- ENVI DEM Extraction, Module of ENVI;

In terms of the accuracies of DTMs, Ortho Engine of PCI Geomatica is widely used (Kääb, 2002; Toutin, 2002; Chrysoulakis *et al*., 2004; Cuartero *et al*., 2004, 2005; Eckert *et al*., 2005). Despite the setback of not being able to process portions of images prior to its geometric corrections, the PCI geomatica can achieve an accuracy level of ±15 and ±15-25m Root Mean Squared Error (RMSE) in the horizontal and vertical directions respectively depending on the nature of the terrain and distribution of GCPs.

ERDAS imagine used to process about 55 stereo data of level 1A data produced a poorer RMSE of ±27m (Cuartero *et al*., 2004; Trisakti and Carolita, 2005). The inefficiency of this software was attributed to the lack of a specific model to process ASTER level 1A stereo data (Deilami *et al*., 2012; Toutin, 2008).

ASTER DTM module developed by SulSoft, the official ENVI distributer in Brazil also has the capability of processing ASTER data of both level 1A and 1B stereo pairs with accuracies of ±17m (Cuartero *et al*., 2005).

DMS software is mostly suitable for photogrammetric mapping purposes obtaining accuracies of ±15-25m (Hirano *et al*., 2003).

Furthermore, SilcAst, of Sensor Information Laboratory Corp., Japan can generate DTM of either level 1A or level 1B at a good and better accuracy of about 6.1m RMSE if compared to 40 Independent Check Points (ICPs). However, there is not much information as to how the algorithm works by enhancing its accuracy level and also, the SilcAst does not accept GCPs which can serve as an input for refinement (Toutin, 2008).

Among the discussed softwares, ENVI is one of the most used and preferred. Lee *et al*. (2008) used the method of automated stereocorrelation in ENVI 4.1 to derive DTMs over an area of 2.15×10^5 Ha using ASTER stereo images to obtain horizontal accuracy of ±7m and vertical accuracy of ±20 m.

2.3 Interpolation and DTM Production

Many factors can affect the production of quality DTMs. These Factors include: the source of elevation data, the type of interpolation algorithm used in converting the data into gridded raster and the land cover of the area (Miller, 2011). Collecting elevation data from an entire study area could be tedious and expensive. In view of that strategically dispersed sample data points from the area or surface could be selected to make predictions for the unknown locations. Interpolation therefore allows the individual to predict values for unsampled points from a limited sample of the entire data points of an area. The purpose of interpolation is to establish regularly spaced set of elevation values that could adequately represent the topography of the terrain, from a limited and sometimes unevenly spaced sample points. The common interpolation techniques include: The Inverse Distance Weighted (IDW), Natural Neighbour (NN), Spline, and Kriging. Each of these techniques have their own advantages and setbacks on various terrain surfaces and users always have varying preferences for each.

Lerberl (1973) suggested that a decision on choosing an interpolation technique could depend on one's intuition, logical considerations and experience. Lee (1991) also in his conclusions made it clear that when one wants to provide accurate information about the topographic structures of the earth, there is always the need to provide a correct middle ground through a trial and error experiment.

According to Lam (1983) there exist no superior interpolation algorithm for all purposes and that the choice of a particular interpolation algorithm should depend on the data type, degree of accuracy expected and computational efficiency.

2.4 Interpolation Types and Methods

There are a number of interpolation methods in use. However, the ones utilized in this research includes: Inverse Distance Weighting (IDW), Spline, Kriging, and Natural Neighbour (NN). When assessing the essential aspects of an ideal interpolation method, Watson (1992) claimed the method must be exact, continuous and smooth, local and also adapt to different densities and distributions of data. In view of that, the algorithms of IDW, Spline, Kriging, and NN possesses such qualities that would be useful in performing various interpolations for analysis.

Interpolation methods can be classified into three groups (Hengl *et al*, 2009):

a. Exact interpolators relying on a smoothing effect where the interpolator preserves the values at the actual measured data points whiles an approximate method uses the measured values obtained by calculating the predicted surface. Mostly this is done in order to achieve surfaces more appealing to the user.

b. Local or global interpolators using a proximity effect. Global interpolators use all the data points in predicting the entire area whereas local interpolators break the entire sample area into smaller pieces before using it for its predictions.

c. Stochastic assumptions observe the distance between data points and also applies autocorrelation among the measured points.

Inverse Distance Weighting (IDW) is a simple and exact form of interpolation which estimates data values by averaging a number of known points within an area. This method tries to identify areas of influence within a search area where measured data points should be considered. The formula can be adjusted to assign more weights to points that are closer to the measured data points and less weight to points that are further apart. The formula for the interpolated value Z(Xo,Yo) is given by :

$$Z(Xo,Yo) = \sum_{i=0}^{n} \lambda i \times Zi \tag{2.1}$$

where $\lambda i = (1 / di^{\beta}) / \sum_{i=0}^{n} (1 / di^{\beta})$, $\beta > 1$

Where λi is the weight for neighbour i

In order to ensure unbiasedness $\sum_{i=0}^{n} \lambda i = 1$

Zi is the measured sample data point.

di is the distance between the known and unknown sampled data point.

β is the parameter used in adjusting the weights. The higher the β the less relevant the distant point is whereas, the smaller the β, the more relevant the distant point is.

The spline is also an exact form of interpolation that tries to reduce the general curvature of the surface. This method utilizes a mathematical function that passes through all the measured data points thereby, resulting in the smoothness of the surface. The mathematical function is given by:

$$Z (xo, yo) = a^{1} + \sum_{i=1}^{n} Wi \times R(Vi) \tag{2.2}$$

Where Z (xo, yo) is the interpolated value and a_1 is a constant.

R(Vi) is the radial basis function (Mitasova and Hofierka, 1993) given by:

$R(Vi) = -[E_1(Vi) + \ln(Vi) + C_E]$ where $Vi = [\varphi \times \frac{ho}{2}]^2$

where $E_1(Vi)$ is the exponential integral function C_E =

0.577215 is Euler constant φ is generalized tension

parameter

And ho is distance between the new and interpolation point.

Kriging is a geostatistical and stochastic method of estimating surfaces using known data points and the semivariogram to predict points in areas that are unknown. The kriging method is similar to the IDW in that, it make use of a weighting system in using weighted mean of known points in estimating unknown points. However, the difference basically lies in the specification of the weight in kriging which does not only consider the distance between measured points but also variations between measured points by using statistics in order to efficiently predict the unknown areas (Eberly *et al*. 2004). The mathematical formulae can be given as:

$$Z(Xo) = \sum_{i=1}^{n} \lambda i \; Z(Xi) \qquad (2.3)$$

For the weight to be unbiased, $\sum_{i=1}^{n} \lambda i = 1$ and also the variance has to be minimum. Minimum variance Z (Xo)is given by $\partial^2 = \sum_{i=1}^{n} \lambda i \; \gamma(Xi, Xo) + \Phi$ and can be obtained when $\sum_{i=1}^{n} \lambda i \; \gamma(Xi, Xj) + \Phi = \gamma(Xj, Xo)$ For all j

Where $\gamma(Xi, Xj)$ is the semivariance of Z between the sampling points Xi and Xj $\gamma(Xi, Xo)$ is the semivariance between the sampling point Xi and the unvisited point Xo Φ is a Lagrange multiplier required for minimization.

Natural Neighbour (NN) interpolation method functions on the concept of Voronoi diagram and the Delaunay triangulation. It tries to find the closest measured sample data points to an unknown point (Garnero & Godone, 2013). NN utilizes the Voronoi diagram to measure areas "stolen" from a defined sets of neighbourhood and this areas serve as the weights for estimating the average (Dianne and Peter, 2002)

2.5 Interpolation Error

As part of the quality of the terrain model generated, the interpolation technique used in modelling the raster terrain from a number of scattered sample dataset is likely to introduce some errors. Quality assessment is therefore a very important parameter when considering the performance of various interpolation algorithms in the production of DTMs and this heavily depends on statistical methods. The possible, preferred and most common used statistics for this purpose are the Root Mean Squared Error (RMSE) and Mean Absolute Error (MAE) with respect to reference data (Podobnikar, 2009).

The RMSE and MAE are mathematically expressed as:

$$RMSE = \sqrt{\frac{(Z_{DEM} - Z_{Ref})^2}{n}} \qquad (2.4)$$

and

$$MAE = \sum \frac{| Z_{DEM} - Z_{Ref} |}{n} \qquad (2.5)$$

Where Z_{DEM} is elevation of measured DTM

Z_{Ref} is the actual measured elevation with a higher accuracy and

n, number of elevation points for checking

Cuartero *et al*. (2004) proposed, accuracy estimation of the model could be obtained by comparing DTM data with a set of check points or reference system that has been acquired through a high precision method. The most common source of this check points or reference system is the digital topographic map which has been generated with a conventionally high and acceptable standard of accuracy or high resolution image pair(s). Spot heights from accurate topographic maps could be used as check points, provided some field data verification is first done to assess results and verification of conforming features through the overlay of ground control points (Xiong Ping, 2003). In the situation where GCP are used, the accuracy of the absolute DTM would highly depend on the accuracy, number and distribution of the control points. For 12 to 25m previous accuracy, control data from 1:50,000 topographic map should be enough (Toutin, 2008).

2.6 Error Analysis of Previous Works

Many studies have been conducted in assessing the quality of the DTMs. Komeil *et al* (2015) determined the accuracy of DTMs by comparing the elevation of some points with true elevation values. The number of ground elevation values used were 20 and this yielded a mean and RMSE of ± 12.60m and ± 14.86m respectively which is actually less than 15m pixel size of an ASTER image. Cuartero *et al* (2004) studied the accuracy of DTMs generated through the process of automatic stereo-matching. The terrain on which the study was performed was a complex topography with steep slopes and flat surfaces. The results from the study indicated a RMSE value of ±13m which was less than an ASTER image pixel size of 15m. Xiong Ping (2003) also generated a DTM from an ASTER image pair through an empirical way and on a mountainous terrain with the results showing an accuracy of ±28m. Kääb (2002) generated DTMs from ASTER data and yielded an accuracy of ± 60m for rough mountain topography and ±18m for its subsection which entailed moderately mountainous terrain. Toutin (2008) reviewed a number of research works on the basic characteristics of stereoscopy and its application to the ASTER in DTM generation and concluded that a standard DTM could produce a geopositioning and elevation accuracy of ±10 to ±30m depending on the number and quality of GCPs used. Eckert *et al* (2005) also stated that with accurate and well distributed GPS, it was possible to generate DTMs with RMSE between 15m and 20m for hilly terrain and about 30m for mountainous terrain however, DTMs are very accurate in nearly flat areas and also on smooth slopes to within ±10m.

These researches by various authors therefore suggests that, during the generation of DTMs from an ASTER dataset, a vertical accuracy of up to ±30m (Eckert *et al*, 2005; Xiong Ping, 2003; Toutin, 2008) could be achieved for mountainous areas however, for flat and smooth sloping areas a better result less than ±15m (Cuartero *et al*, 2004; Komeil *et al*, 2015; Eckert *et al*, 2005) is obtainable.

Studies have shown that ASTER data should prove convenient and sufficiently accurate (Lang and Welch, 1998) for topographic mapping of high relief terrains having scales from 1:50,000 up to 1:100,000 with 40m contour interval or larger (Nikolakopoulos *et al*, 2006).

This study focuses on performing various interpolation algorithms on an ASTER dataset in order to make analysis and verify which interpolation algorithm when performed would closely represent the topographic map for each landform type.

CHAPTER THREE

MATERIALS AND METHODOLOGY

3.1 Study Area

The four interpolation algorithms were applied to three datasets in different areas. The first study area is Edwenase-Kwadaso which is a suburb of Kumasi in the Ashanti Region. This area lies on latitude (6.42° to 6.49°)N and longitude (1.34° to 1.42°)W with an average elevation of about 284m above mean sea level. This area Figure 3.1(a) is selected because the terrain is mostly flat planes especially in the agricultural areas (Sadick, 2015)

The second region investigated is KNUST campus on latitude (06° 35´ to 06° 45´)N and longitude (01° 30´ to 01° 35´)W and about 7 square miles in area. It is about 13km to the east of kumasi, the regional capital of Ashanti Region. The topography of KNUST campus and its surrounding towns Figure 3.1(b) is chosen because the topography is generally undulating with elevation ranging from about 110m to about 280m.

The third, lake Bosomtwi and surrounding towns in Figure 3.1(c) is on latitude (06° 26´ to 06° 30.3´)N and longitude (01° 24.5´ to 01° 30´)W. It is about 30km and south-east of Kumasi, the regional capital of Ashanti Region. Bosomtwi region is also chosen because the topography around the lake is surrounded by a complex slight irregular, circular and continuous depression which has an outer ring of minor mountainous topographic heights with elevations ranging from 150m up to about 700m.

MAP OF STUDY AREA

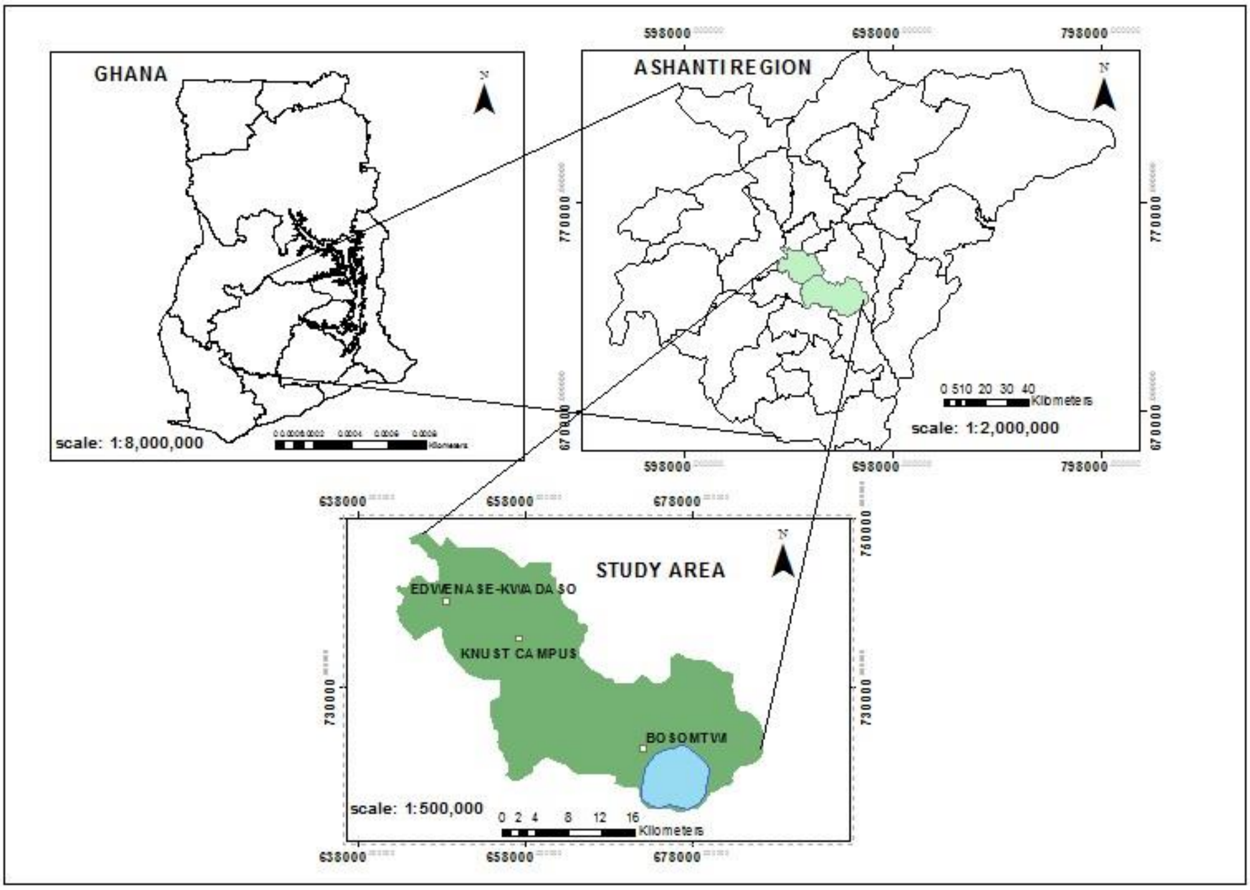

Figure 3.1: Study areas showing Edwenase-Kwadaso (Agricultural Station), KNUST Campus and Bosomtwi District from the map

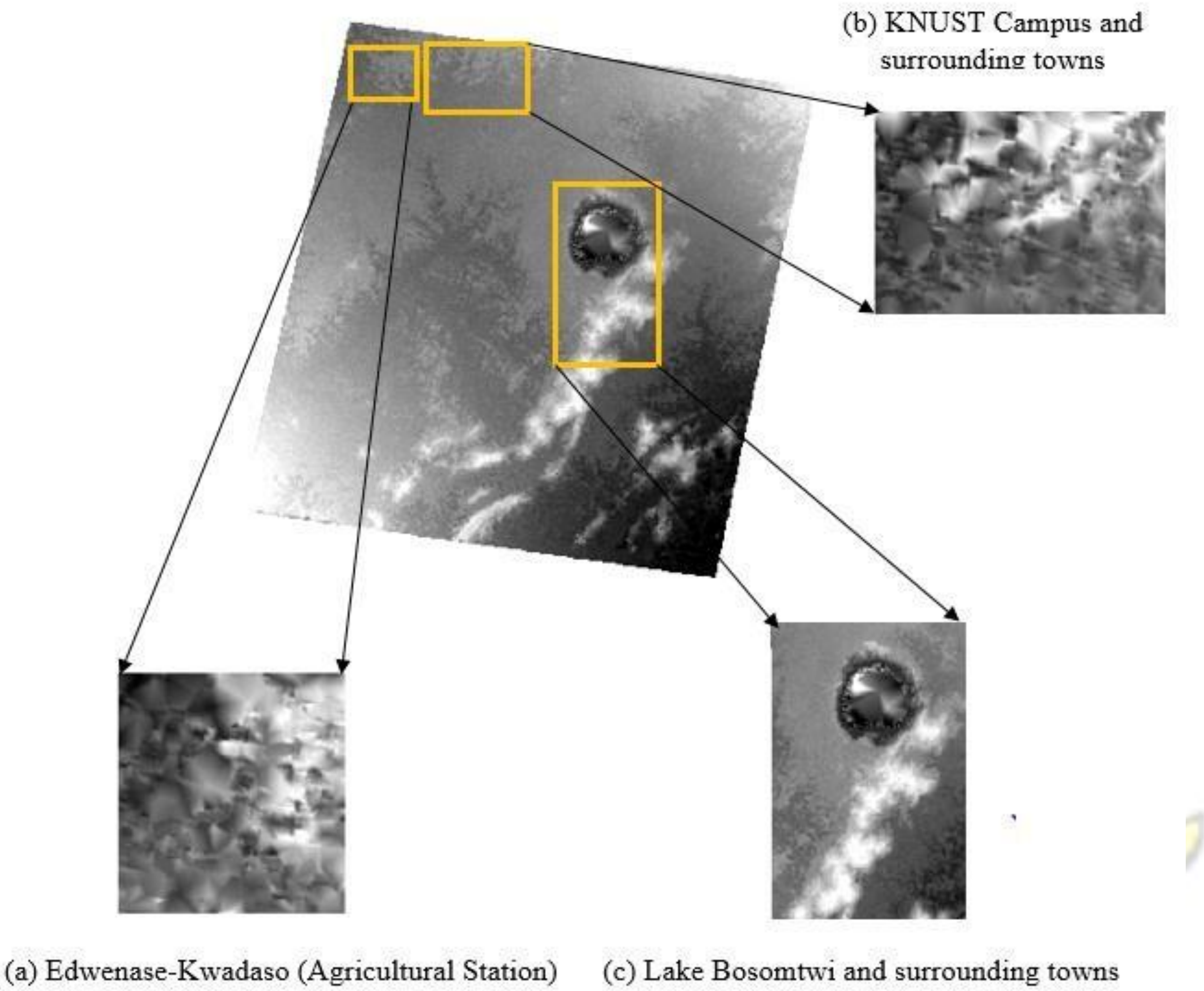

Figure 3.2: Showing the study areas from the ASTER DTMs

3.2 Materials

To produce the DTM ASTER_L1B image was obtained from NASA's Earth Observing System (EOS). This image has 14 bands where the 3N and 3B images within the visible and near infrared regions are used for the generation of the DTM. The format of the image is the Hieratical Data Format (HDF) and this referenced to the Universal Transverse Mercator (UTM) projection system which is on WGS 84 ellipsoid. The software ENVI which has the power to produce DTMs is utilized to produce the DTM.

3.3 Methodology

Introduction

The generation of DTM by automated stereocorrelation is one of the most suited methods for generating DTMs from satellite stereo images. Stereocorrelation technique provides a computational and statistical means of generating DTMs automatically from registered stereo image pairs (Ackermann, 1984; Ehlers and Welch, 1987; Lang and Welch, 1999). The primary advantage of stereocorrelation is automatic image matching (Lee *et al*, 2008). There are three basic steps in creating DTMs with acceptable results. These include the epipolar image creation, image matching and DTM geocoding methods. ASTER instrument has two forms of data, the Level-1A and Level-1B data. Level-1A has full resolution but the radiometric coefficients, the geometric coefficients and other auxiliary data has not been applied to maintain the original data values however, Level-1B has these coefficients applied for radiometric calibration and geometric resampling. The methodological flow used in current work is shown in Figure 3.3.

DESIGN OF THE WORKFLOW

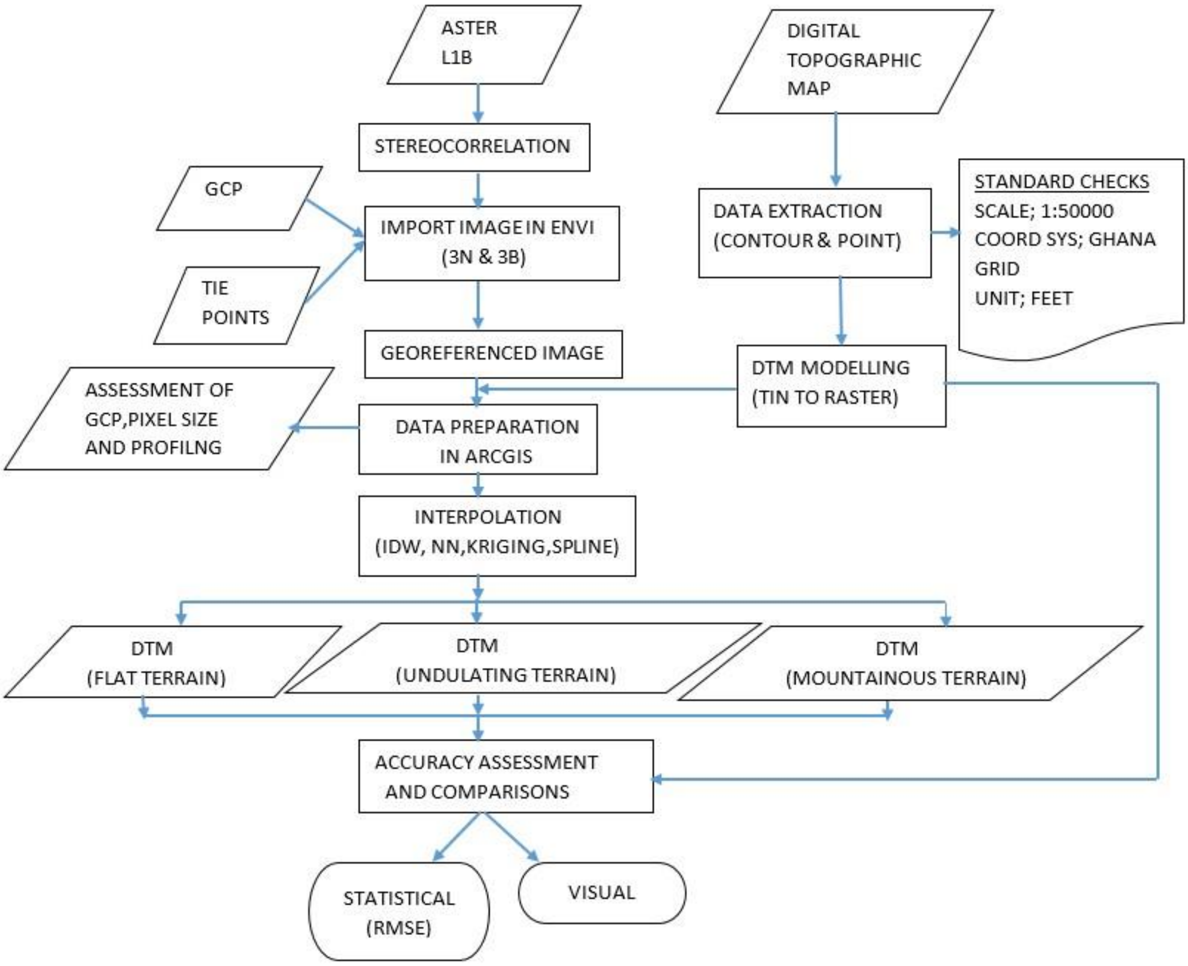

Figure 3.3: Methodology used in DTM generation and Assessment

3.3.1 DTM Generation

To begin with the generation of the DTM, the two stereo pair bands (3N and 3B) of the ASTER were imported into the ENVI 5.1. This stereo pair images contain Rational Polynomial Coefficients (RPC) which generates tie points to calculate the relationship between the stereo pair images. This therefore paves the way for the manipulation of GCPs and Tie points. The provision of ground controls ensures the absolute orientation of the terrain model thereby decreasing the error involved with the elevation values. According to Toutin (2002) and San *et al* (2005), increasing the number of ground control points enables a reduction in error propagation of the terrain model. Also as stated by Hirano *et al* (2003), a minimum of eight evenly distributed GCPs are sufficient for DTMs generation. For this study, a total of ninety

(90) GCPs covering three different terrain types were selected from the available topographic map and/or GPS surveys. These control points were evenly distributed and were interactively entered into the DTM generation process. The distribution of GCPs is shown in figure 3.4.

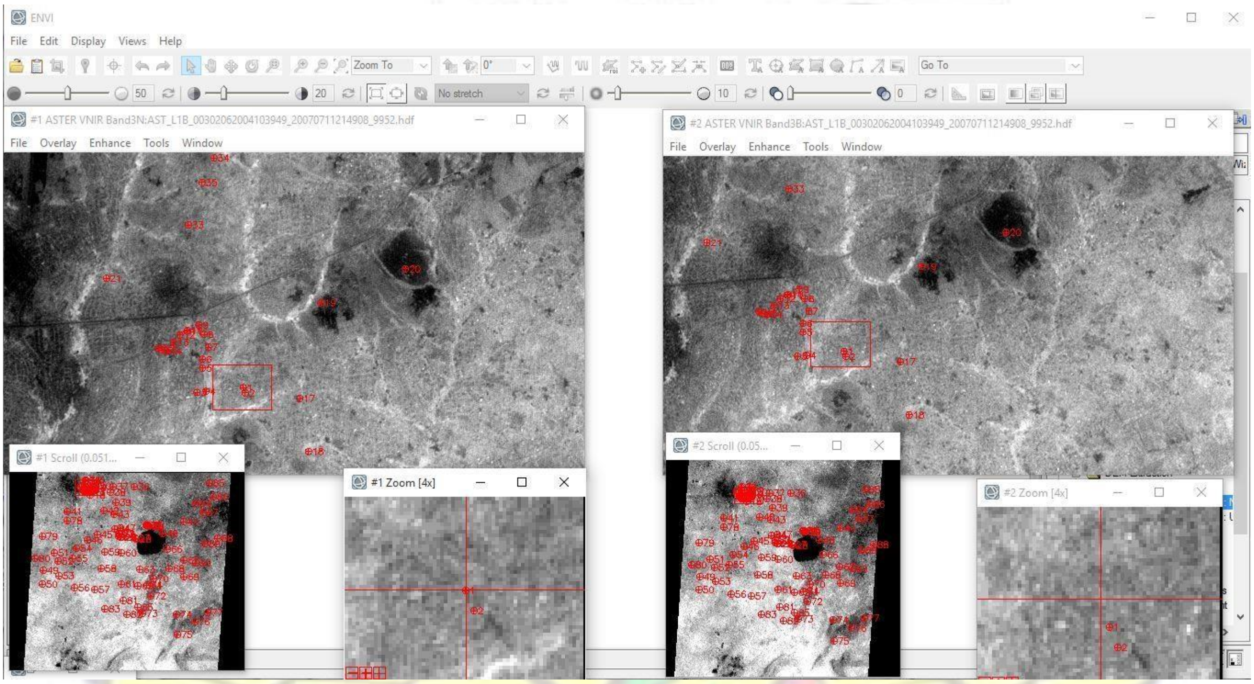

Figure 3.4: Distribution and location of GCPs within the ENVI DTM Extraction Wizard

3.3.2 Tie Points

Generation of tie points is very crucial for the generation of DTMs. The tie points define the epipolar geometry and also create epipolar images which are used in the extraction of DTMs. For this study, 25 tie points were chosen automatically to suit the terrain features within the image. A Search Window Size and a Moving Window Size of 101 and 19 were chosen respectively and these values were sufficiently enough for the stereo pair. The Moving Window defines an area within the Search Window that is used to scan and find reliably similar topographic feature match for a tie point placement. Increasing the tie points, search window size, as well as the moving window size increases the reliability of the matching and for this study, the selected parameters appeared reasonable for the 15m resolution ASTER data. The generated tie points examined and edited to eliminate parallax on y are as shown in Figure 3.5.

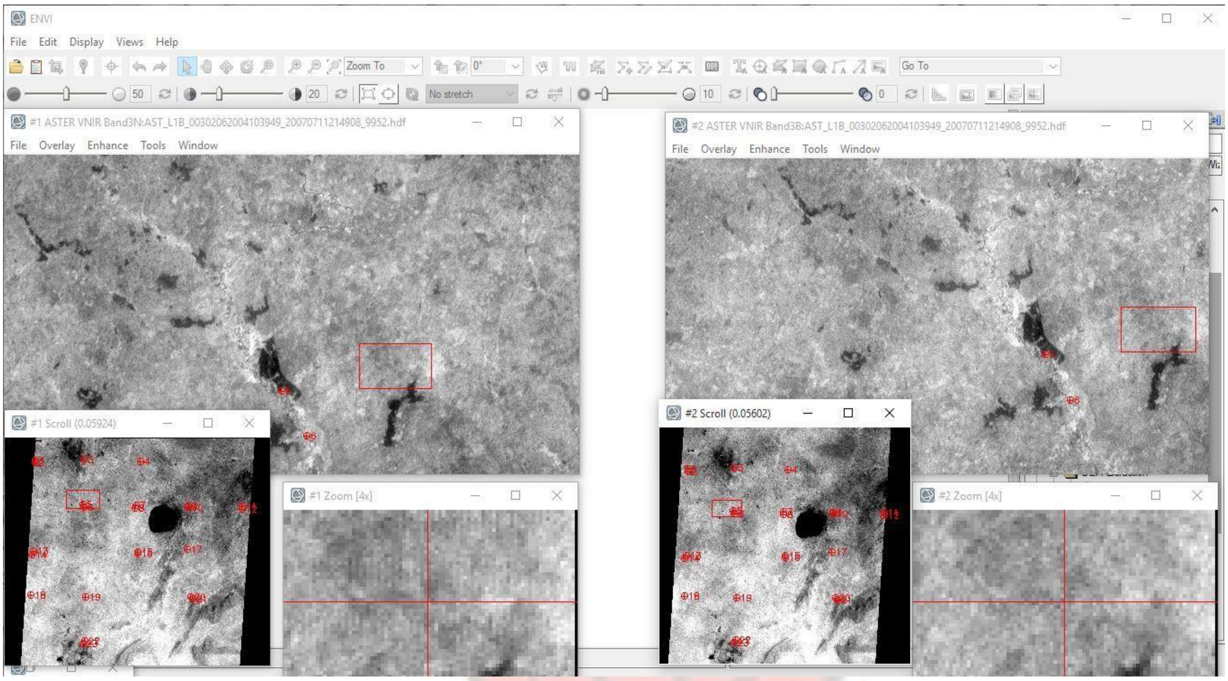

Figure 3.5: Distribution and location of tie points within the ENVI DTM Extraction Wizard

3.3.3 DTM Extraction Parameters

After the reduction of the y parallax, the various thresholds of the epipolar parameters were examined. Here, the reducing epipolar factor was set to 1 to ensure that the epipolar image has the same resolution as the input images. The epipolar images were processed and projected to the UTM, zone 30 north on the WGS-84 datum with the X, Y pixel sizes being set to 15m. In general, the correlation coefficient with values between 0.65 and 0.85 is considered good and for this study hence a correlation threshold of 0.70 was used. The moving window which determines the region or area to perform the image matching was set to 5×5 in order to yield a more precise and reliable image matching result. To best represent the terrain in the DTM production, the terrain relief was set to moderate with a level 3 in the terrain detail. This was to help achieve a pyramid image composed of several layers with each representing the same image but with a specified spatial resolution.

The resultant DTM generated from ASTER-L1B data in grey coding mode with 15m resolution, is shown in Figure 3.6.

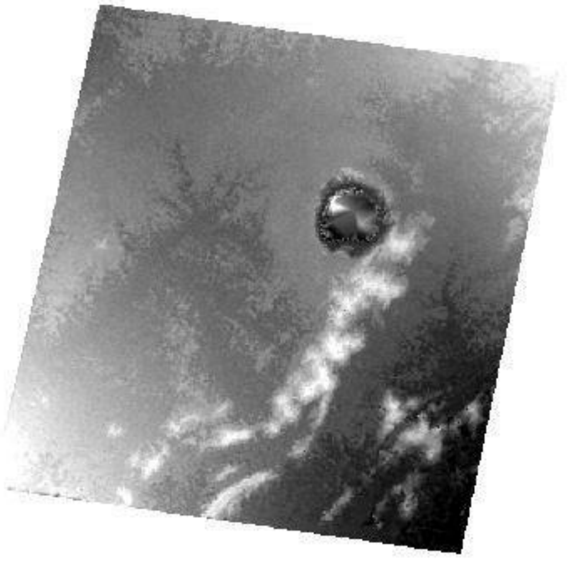

Figure 3.6: DTM generated from ASTER stereo image with a grid interval of 15m

3.3.4 Ground Control Points Assessment.

In checking the accuracy of the GCPs, one of the experiments that was carried out was to vary the GCPs covering an area of 3600sq. kilometres and this resulted in different RMSE's (Table 3.1):

Table 3.1: Number of GCPs and their respective RMSE values

SATELLITE IMAGE	RMSE OF GCPs			
	40 Points(m)	60 Points(m)	80 Points(m)	90 Points(m)
ASTER STEREO PAIR (3N AND 3B)	±17.940	±15.135	±9.548	±9.239

Source: Authors Construct.

In all, RMSE values were computed from the generated DTM using various number of check points. Forty (40), sixty (60), eighty (80) and ninety (90) ground controls were used for the assessment of both stereo images. The RMSE for 40 ground controls came out to be the highest whiles that of the 90 ground controls came out to be the lowest and for that matter good for DTM generation.

3.3.5 Image Resolution Assessment

For vertical accuracy assessment of the DTM, the pixel sizes of the DTM was varied. 90 spot heights as GCPs were selected from the topographic map and then used in generating the DTM. The pixel sizes were then varied for 15m, 20m, 25m and 30m and this resulted in varying RMSE Table 3.2. The maximum and minimum error gives the maximum and minimum residual values of the reference information (Ping, 2003) whiles the mean error gives the mean residual error for the 3D measurements.

Table 3.2: Varying pixel sizes of the generated ASTER-DTM and their respective RMSE values

PIXEL SIZE OF GENERATED ASTER-DTM	90 GCPs			
	15 m	20 m	25 m	30 m
Minimum Error (m)	-15	-27	-22	-24
Maximum Error (m)	30	29	31	28
Mean Absolute Error (m)	7.050	12.875	12.725	13.000
RMSE	±9.239	±14.917	±14.681	±15.129

Source: Authors Construct

The results reveals that the RMSE for the 15m pixel size DTM is 9.239 which was the least RMSE obtained and considered good for further analysis (Toutin, 2001; Hirano *et al*, 2003).

3.3.6 Profile Assessment

As part of the accuracy assessment of the generated DTM, a profile graph was plotted to show the changes in elevations of the ASTER-DTM with respect to that from the contour map. The elevation differences through the transect line drawn from A to B Figure 3.7 and

Figure 3.8 shows a good correspondence between the topographic map DTM and the ASTER-DTM. This is revealed in the elevation values of the ASTER-DTM (black solid line) almost coincidence with the topographic map DTM (red solid line).

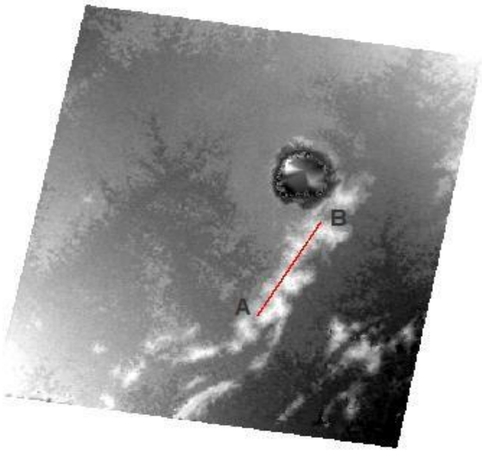

Figure 3.7: Showing profile drawn from point A to B

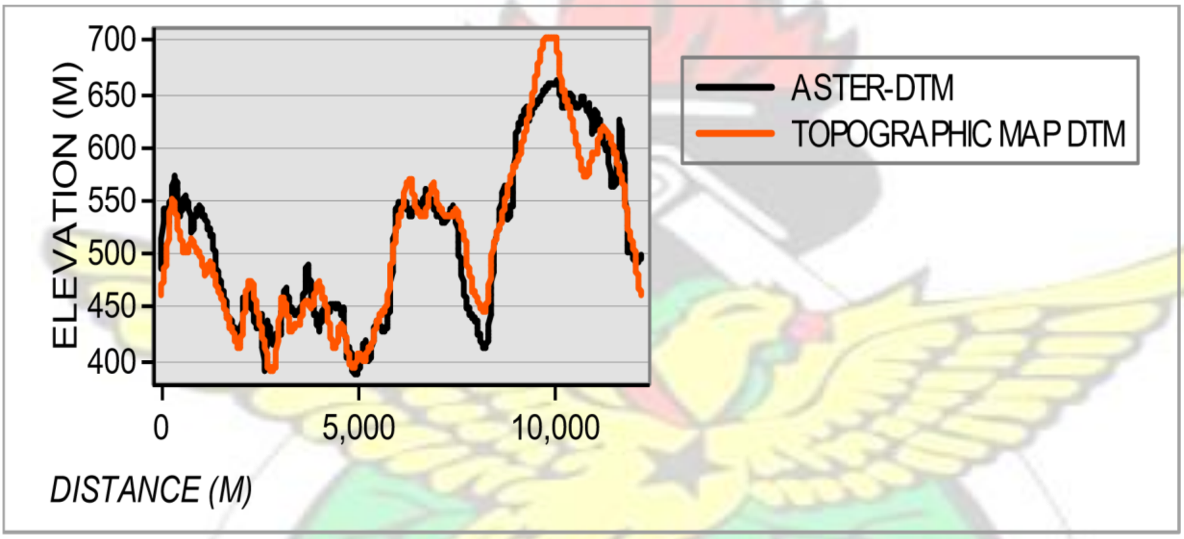

Figure 3.8: Profile of ASTER-DTM and Topographic map DTM in black and red respectively

3.3.7 Contour Derived DTM

ESRI ArcGIS was used to convert contours from the topographic map to elevation points (Peng *et al*, 2004). Mostly, in the derivation of DTMs from contours, elevation values could somewhat tend to be generalized, thereby not reflecting some key features of the actual surface. In order to avoid or reduce such occurrences, it is best to supplement the contours with point measurement of elevations (Nelson *et al*, 2009).

When using the contour and point features from the topographic map, it was necessary to verify the quality of the map (Forkuo, 2008; Forkuo, 2010). For this study, the following conditions were identified and tested; map scale (1:50000); coordinate system (Ghana grid); map units (feet) and grid interval (1000). With the extraction of contour and elevation features, grounds for interpolation was then prepared for the generation of DTM within the ESRI ArcGIS environment to serve as a standard in our analysis.

In order to test the performance of the generated DTM from ASTER, a contour map was generated with 50 feet interval since each feature was viewed as a pixel of 15m. The contour lines were then overlaid onto the original topographic contour map and the two showed a good visual correspondence.

To enable easy manipulation of the digitized contour datasets with other terrain models, it was necessary to structuralize the topographic map into a regular raster format. To generate a DTM from the 2D and elevation observation, a TIN model was first generated and then converted to raster form as DTM (Forkuo, 2008), (Figure 3.9 to 3.11).

(a) 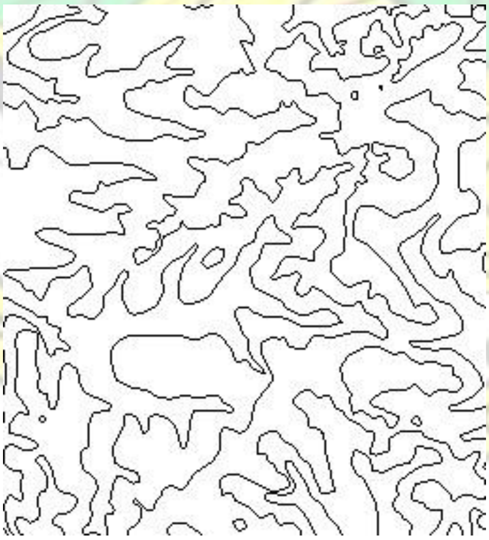 (b) 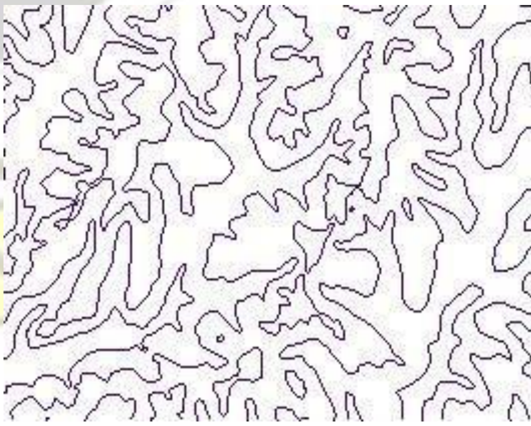

(c) 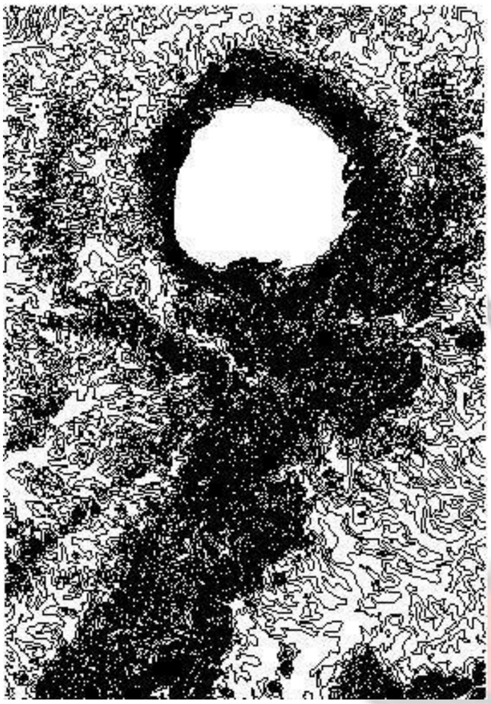

Figure 3.9: Sample of digitized topographic map of the various study areas: (a) EdwenaseKwadaso (Agricultural Station). (b) KNUST campus and surrounding towns. (c) Lake

Bosomtwi and surrounding towns

(a)  (b) 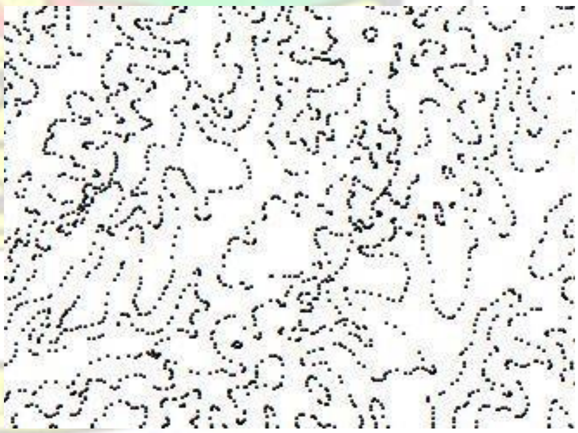

(c) 

Figure 3.10: Extraction of elevation from contour lines of the various study areas : (a) Edwenase-Kwadaso (Agricultural Station). (b) KNUST campus and surrounding towns. (c) Lake Bosomtwi and surrounding towns

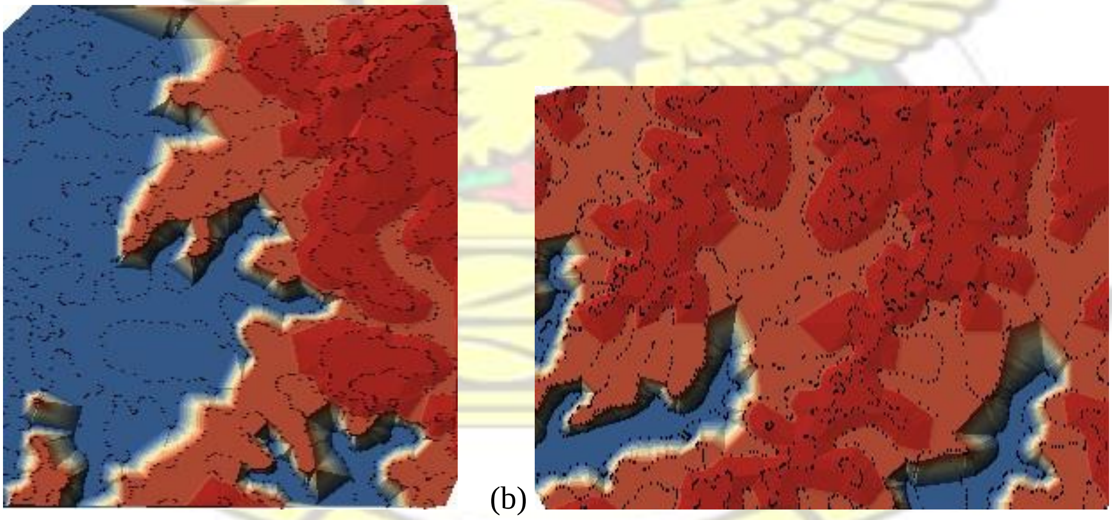

(a) (b)

(b) 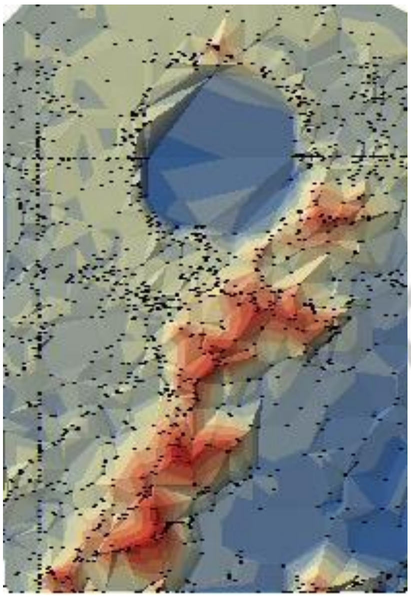

Figure 3.11: Generated TIN models of the various terrain elevations as created in ESRI ArcGIS : (a) Edwenase-Kwadaso (Agricultural Station). (b) KNUST campus and surrounding towns. (c) Lake Bosomtwi and surrounding towns

3.3.8 Interpolation

After the generation of the ASTER-DTM the data was imported into the ESRI ArcGIS environment for further analysis. In the preparation of the ASTER dataset for interpolation within the ESRI ArcGIS, the intersect tool was used to extract point elevation values corresponding to both the rasterized topographic map and the generated ASTER-DTM, as well as the geographic positions (x, y) of the points. The intersect tool computes the geometric intersection of the input features that overlaps and writes the overlapping layers to the output feature class. The elevation values were plotted to a shapefile from which DTM surfaces were generated using four different interpolation methods namely IDW, kriging, NN and spline.

The cell size and search radius for the IDW, NN, kriging and spline were set to 15 and 12 respectively. The cell size determines the extent or size with which output raster should be created whereas the search radius specifies which of the input points would be used to interpolate each cell value in the output raster. The power (exponent of distance) for the IDW was specified as 2 to control the significance of surrounding points on the interpolated value as higher powers result in less influence from distant points.

Tension was selected for the spline type and a weight of 0.1 was used. The tension tunes the stiffness of the interpolant according to the character of the modeled phenomenon and the weight parameter influences the character of the surface interpolation. The ordinary kriging method which assumes no fixed mean or trend was used with the spherical model of the semivariogram.

3.3.9 Check Points

Accuracies of the generated DTMs were evaluated using various number of accurate and well distributed GCP from spot heights and/or GPS systems. Statistical procedures as well as visual analysis were used for comparative assessment of the interpolated surfaces. RMSE is used to calculate the deviation of the interpolated elevation values from corresponding check point elevations that has been selected. In comparing the check points, spot heights within the extent of the topographic map were selected. The selection criteria included all terrain characteristics such as mountainous areas, slope surfaces, flat areas, road intersections and public facilities. 40 check points were randomly selected from the topographic map and used to help evaluate the vertical accuracy of the DTM generated. The residuals represent the difference between the interpolated DTM elevations and their corresponding check point elevations. 25 GPS measurement points were collected from the KNUST campus study area whereas 40 spot heights were also collected from the topographic map for the calculation of the RMSE and MAE for both Edwenase-Kwadaso and Bosomtwi study areas. The point densities of Edwenase-Kwadaso, KNUST campus and Bosomtwi study areas were 61.49 points per km^2, 62.30 points per km^2 and 141.64 points per km^2 respectively.

CHAPTER FOUR

RESULTS AND DISCUSSIONS

4.1 Results

The results of interpolated DTMs are shown in Figure 4.1, Figure 4.2 and Figure 4.3. Figure 4.1 shows the rasterized topographic map (a) used as standard as against the interpolated rasters using IDW (b), Kriging (c), Natural Neighbour (d) and Spline (e) derived from ASTER for a flat terrain.

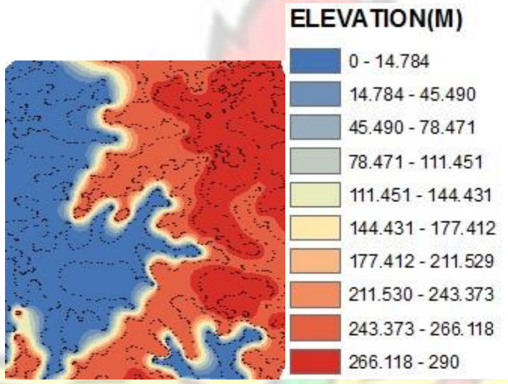

(a) RASTERIZED TOPOGRAPHIC MAP

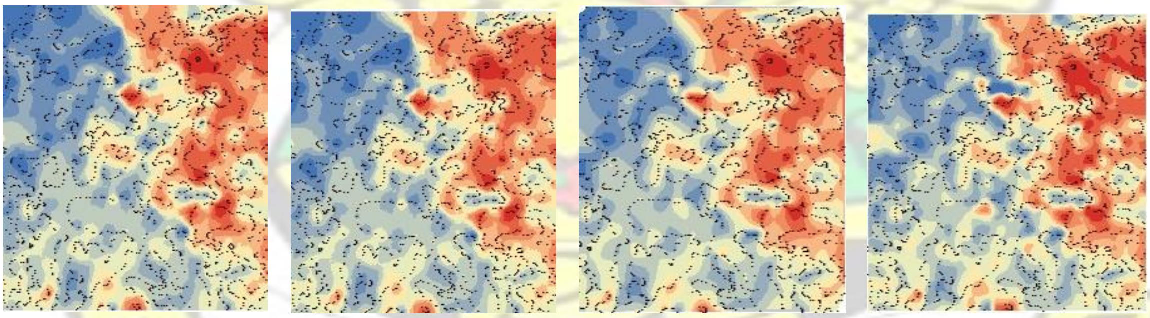

(b) IDW (c) KRIGING (d) NATURAL NEIGHBOUR (e) SPLINE

Figure 4.1: IDW, Kriging,NN and Spline DTMs at 15m grid spacing of Edwenase-Kwadaso (Agricultural Station)

Figure 4.2 shows the rasterized topographic map (a) used as standard as against interpolated rasters using IDW (b), Kriging (c), Natural Neighbour (d) and Spline (e) derived from ASTER for an undulating terrain.

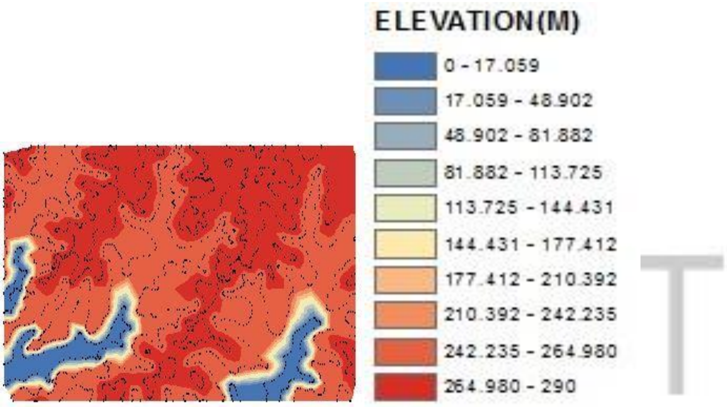

(a) RASTERIZED TOPOGRAPHIC MAP

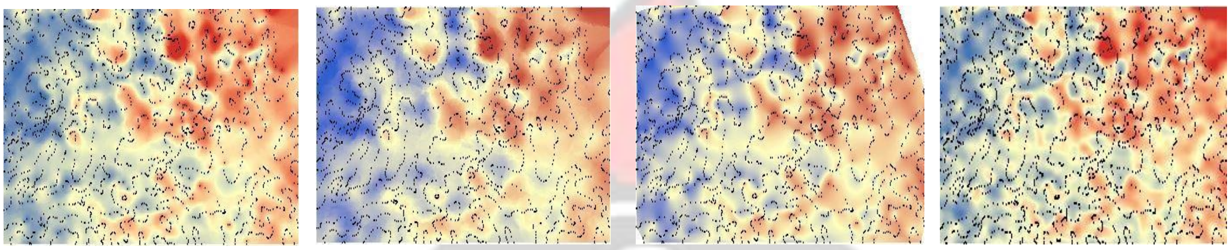

(b) IDW (c) KRIGING (d) NATURAL NEIGHBOUR (e) SPLINE

Figure 4.2: IDW, Kriging,NN and Spline at 15m grid spacing of KNUST campus and its surrounding regions

Figure 4.3 shows the rasterized topographic map (a) used as standard as against interpolated rasters using IDW (b), Kriging (c), Natural Neighbour (d) and Spline (e) derived from ASTER for a complex mountainous terrain.

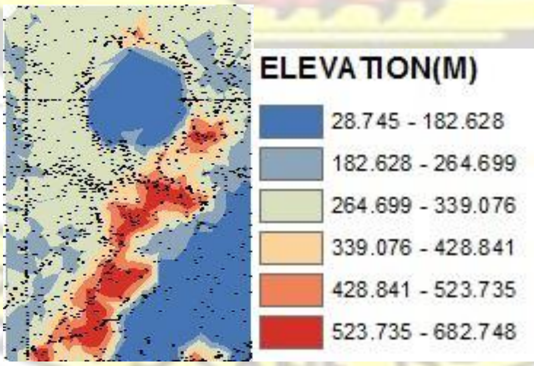

(a) RASTERIZED TOPOGRAPHIC MAP

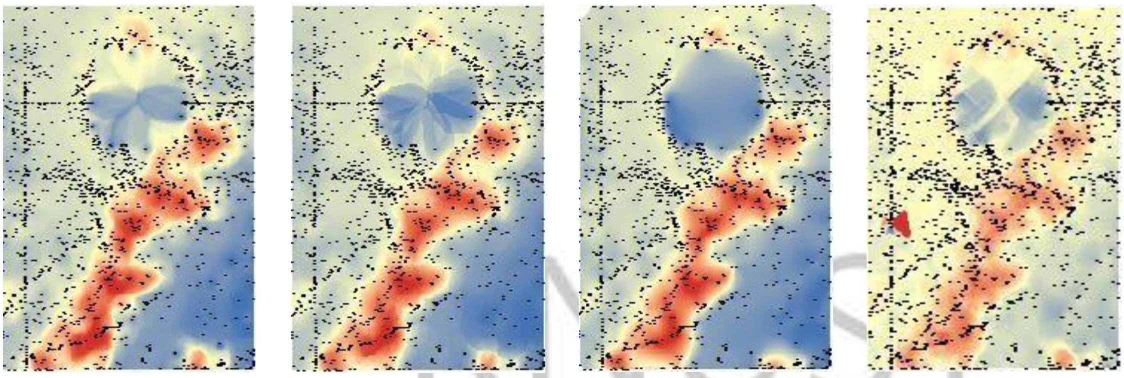

(b) IDW (c) KRIGING (NEIGHBOURd) NATURAL (e) SPLINE

Figure 4.3: IDW, Kriging,NN and Spline DTMs at 15m grid spacing of lake Bosomtwi and its surrounding regions

ESRI ArcGIS module ArcScene creates a very good platform for viewing and analyzing two or more layers of data in different dimensions. A visual comparison of the four interpolation results with respect to the reference topographic map is made using the ArcScene.

In order to assess quantitatively the accuracy of the ASTER-DTM before performing the interpolation, 40 evenly distributed spot heights were selected from the topographic map and the results are shown in Table 4.1. These points were to serve as check points in computing the residual between the elevation points extracted from the ASTER data and spot height points

Table 4.1: Accuracy assessment of generated DTM from ASTER

GENERATED ASTER-DTM	**NUMBER OF GCP(90)**
MAE	± 7.050
RMSE	± 9.239

The most common, preferred measure of DTMs accuracy is the MAE and the RMSE (Smith *et al*, 2004; Weibel and Heller, 1991). The MAE indicates the mean residual error for all 3d reference observations (Ping, 2003) whereas the RMSE indicates the quality of the generated

DTM (Ping, 2003). The higher the RMSE value, the poorer the results. The MAE and RMSE values obtained are presented in Table 4.2 to Table 4.4.

Table 4.2: Accuracy assessment of the four interpolating algorithms on the Flat terrain (Edwenase-Kwadaso (Agricultural Station))

FLAT TERRAIN	**NUMBER OF GCP(40)**			
INTERPOLATION ALGORITHM	**SPLINE(m)**	**NN(m)**	**KRIGING(m)**	**IDW(m)**
MAE	±8.999	±9.102	±9.979	±8.714
RMSE	±11.035	±11.121	±12.108	±10.773

Table 4.3: Accuracy assessment of the four interpolating algorithms on the undulating terrain (KNUST campus)

UNDULATING TERRAIN	**NUMBER OF GCP(25)**			
INTERPOLATION ALGORITHM	**SPLINE(m)**	**NN(m)**	**KRIGING(m)**	**IDW(m)**
MAE	±11.028	±10.963	±11.658	±10.789
RMSE	±13.717	±13.711	±14.835	±13.549

Table 4.4: Accuracy assessment of the four interpolating algorithms on the mountainous terrain (Lake Bosomtwi and surrounding regions)

MOUNTAINOUS TERRAIN	**NUMBER OF GCP(40)**			
INTERPOLATION ALGORITHM	**SPLINE(m)**	**NN(m)**	**KRIGING(m)**	**IDW(m)**
MAE	±14.544	±13.909	±15.241	±14.687
RMSE	±21.721	±19.044	±21.167	±21.632

4.2 Discussions

The accuracy of the ASTER-DTM is ascertained using the elevations of some randomly selected points in the DTM and comparing them with actual ground control points by computing RMSE and MAE, calculated through the difference between the elevations of the ASTER-DTM and the check points. The results Table 4.1 show that the RMSE and MAE of the ASTER-DTM are ±9.239m and ±7.05m respectively. This results indicate that ASTERDTM generated has a resolution less than 15m pixel size of a standard ASTER image.

For this study, four interpolation methods namely IDW, NN, kriging and spline were performed on three terrain types. Visual comparisons of the interpolation techniques reveal that: (Figure 4.2) for the Edwenase-Kwadaso study area which has most of the terrain surface being flat, the IDW method out-performed all the other methods. Statistically also, it has the lowest RMSE and MAE values of ±10.773m and ±8.714m respectively. Spline and NN method were also found to perform quite moderately with the Spline giving a RMSE of

±11.035m, MAE of ±8.999m and NN giving a RMSE of ±11.121m, MAE of ±9.102m. The kriging method was the poorest performer for this landform type with RMSE value of ±12.108m and a MAE of ±9.979m.

Although, all the interpolation methods gave a good estimate of elevation values below the 15m standard ASTER image resolution, they all do not give a good visual representation of the terrain characteristics as given in Figure 4.1 (a) of the rasterized topographic map. Also, all the interpolation methods gave a good estimate of elevation values, better than those of both the undulating and mountainous terrain surfaces.

For an undulating terrain (KNUST), the IDW method out-performed all the other methods with the least RMSE and MAE values of ±13.549m and ±10.789m respectively. NN and spline method were found to perform quite moderately, the NN gave a RMSE of ±13.711m, MAE of

±10.963m and spline gave a RMSE of ±13.717m, MAE of ±11.028m. The kriging method was the poorest performer with the highest RMSE value of ±14.835m and a MAE of ±11.658m.

For a complex mix of mountainous terrain (lake Bosomtwi and the surroundings), NN is the best performer both quantitatively and visually. NN gave the lowest RMSE value of ±19.044m and a MAE of ±13.909m and was found to also yield a good representation of the lake and mountainous regions. Kriging, IDW and Spline methods yielded similar RMSE and MAE values however, kriging seem to have performed better than IDW with spline being the worst for this landform type. The RMSE for kriging, IDW and spline respectively were ±21.167m, ±21.632m and ±21.721m with corresponding MAE of ±15.241m, ±14.687m and ±14.544m.

CHAPTER FIVE

CONCLUSIONS AND RECOMMENDATIONS

5.1 Conclusions

For this work, four interpolation methods were used to generate various DTMs namely IDW, NN, kriging and spline and their accuracies assessed using RMSE and MAE calculated from randomly selected GCPs.

The results showed that vertical accuracy with RMSE value of ±10.771m (MAE= ±8.714m) can be achieved using IDW interpolation for flat lands whereas other interpolation methods though usable would yield worse results. Also IDW represents the landform better than the other three methods investigated.

For a moderately undulating landform, vertical accuracy with RMSE of ±13.549m and MAE of ±10.789m can be achieved using IDW interpolation method as compared to values of

±13.711m (MAE= ±10.963m) to ±14.835m (MAE= ±11.658m) from the other three interpolation algorithms. IDW also gave better visual resemblance of topography than the other methods.

For a complex mountainous landform, elevation RMSE accuracy of ±19.044m (MAE= ±13.909m) can be achieved using NN interpolation method. This method further gives a good representation of the landscape than the other methods but with kriging also performing moderately well (RMSE value of ±21.167m (MAE= ±15.241m))

The conclusion from the studies therefore indicate that, amongst the four interpolation methods (IDW, NN, spline and kriging), IDW should be preferred for flat and undulating terrains, but for a mountainous area, NN should be the preferred method. Additionally, it can be concluded that the vertical accuracy of the IDW interpolation method tends to be more accurate as the terrain becomes more flat and smooth as observed also by Eckert (2005).

5.2 Recommendations

The DTM generated from ASTER-L1B data was useful for interpolation and data quality assessment. However, it is recommended that future work should explore other satellite imagery with stereo capabilities such as SPOT, MOM, IRS, etc. in terms of interpolation and data quality assessment. In this study, a fixed number of points were used for all the interpolation methods. Hence deductions of comparative performance with respect to landform type is based on using a point distribution corresponding to only the topographic map and ASTER DTM. Varying this could well yield an optimum distribution for each interpolation type that could yield best results but this is recommended for a future investigation.

REFERENCES

Ackermann, F., (1984), “Digital image correlation: performance and potential application in photogrammetry.”, *Photogrammetric Record*, 11(64), pp 429-439.

Cuartero A., Felicísimo A.M., Ariza, F.J., (2004),” Accuracy of DEM generation from Terra-Aster stereo data.”, *IAPRS&SIS*, Vol. 35, Part B6, pp 225-260.

Chrysoulakis, N.,Diamandakis,M. and Prastacos, P., (2004), “GIS integration of ASTER stereo imagery for the support of watershed management.” *Global Nest: the International Journal*, 5, pp 1–10.

Cuartero, A., Felici ´Simo, A.M. and Ariza, F.J., (2004), “Accuracy of DEM generation from TERRA-ASTER stereo data”. *International Archives of Photogrammetry and Remote Sensing*, 35(B2), pp 559–563.

Cuartero, A., Felicisimo, A.M. and Ariza, F.J., (2005), “Accuracy, reliability, and depuration of SPOT HRV and Terra ASTER digital elevation models.” *IEEE Transactions on Geoscience and Remote Sensing*, 43, pp 404–407.

De Wulf, A., Constales, D., Stal, C., Nuttens, T., (2012), “Accuracy Aspects of Processing and Filtering of Multibeam Data: Grid Modeling versus TIN Based Modeling.” FIG Working Week 2012, Knowing to manage the territory, protect the environment, evaluate the cultural heritage Rome, Italy, 6-10 May 2012 pp. 1-15.

Deilami, K., Khajeh, S., Bolhassani, N. and Jazireeyan, I., (2012), “Application of ASTER Satellite in Digital Elevation Model Generation:A Review”, *Research Journal of Environmental and Earth Sciences*, pp 1033-1037.

Eberly, S., Swall, J., Holland, D., Cox, B., Baldridge, E., (2004). “Developing Spatially Interpolated Surfaces and Estimating Uncertainty.”, U.S. Environmental Protection Agency, Research Triangle Park, NC 27711, Report No. EPA-454/R-04-004, pp 1–160.

Eckert, S., Kellenberger, T. and Itten, K., (2005), “Accuracy assessment of automatically derived digital elevation models from ASTER data in mountainous terrain.” *ISPRS Journal of Photogrammetry and Remote Sensing*, 26, pp. 1943–1957.

Ehlers, M. and Welch, R., (1987), “Stereo correlation of Landsat TM images.” Photogrammetric Engineering and Remote Sensing.”, 53(9), pp 1231-1237.

ERDAS (2003). ERDAS Field Guide. 7th ed. Leica Geosystems GIS and Mapping LLC,Atlanta, GA, pp. 265-303.

ERSDAC. (2001), Earth Remote Sensing Data Analysis Center, ASTER user's guide partI. General (Ver.3.1), Japan.

Fujisada, H., Bailey G.B., Kelly G.G., Hara S. and Abrams M.J. (2005),”ASTER DEM performance*.”, IEEE Trans. Geosci. Remote Sens.*, 43(12), pp 2702–2714.

Forkuo, E. K., (2010), “Digital Elevation Modelling Using ASTER Stereo Imagery”, *Journal of Environmental Science and Engineering*, 52(2), pp 81-92.

Forkuo, E. K., (2008), “Digital Terrain Modelling in a GIS Environment”. *The International Archives of Photogrammetry, Remote Sensing and Spatial Information Sciences,* 37(B2), pp 1023-1029.

Garnero, G. and D. Godone, (2013), “Comparisons between different interpolation techniques”. Proceedings of the International Archives of the Photogrammetry, Remote Sensing and Spatial Information Sciences XL-5/W3, Feb. 27-28, Padua, Italy, pp 139144.

Hirano.A., Welch R. and Lang H., (2003) “Mapping from ASTER stereo image data: DEM validation and accuracy assessment”. ISPRS J. *Photogramm. Remote Sens*., Vol.57,pp 356-370.

Hengl, T., (2006),” Finding the right pixel size.” Computers &Geosciences 32 (9), pp 1283 - 1298

Hengl T. and Evans I.S., (2009) “Mathematical and Digital Models of the Land Surface”. In: *Geomorphometry: concepts, software, applications.* T.Hengl & H. I. Reuter (eds.): pp.

48-56 .Developements in Soil Science, Vol. 33. Elsevier, Amsterdam.

Jain, D. S., Rao, C. V., Kumar, S. R. and Suresh, S., (2008),” Assessment of DEM mosaic accuracy.”, The *International Archives of the Photogrammetry, Remote Sensing and Spatial Information Sciences.*, Part XXXVII., Part B8, pp 1137 – 1141

Kääb, A., (2002), “Monitoring high-mountains terrain deformation from air- and spaceborne optical data.” *ISPRS Journal of Photogrammetry and Remote Sensing*, 57, pp 39–52.

Komeil, R., Anuar A., Sharifeh H., (2015),” Comparative Analysis Of Aster DEM, ASTER GDEM, And SRTM DEM Based On Ground-Truth GPS Data.” *Jurnal Teknologi (Sciences & Engineering)* 76:1, pp 97–102

Lam, N.S., (1983), “Spatial interpolation methods: a review.” *The American Cartographer*. 10(2): pp 129-149.

Leberl, F., (1973), "Interpolation in Square Grid DTM", *The ITC Journal.*

Lee, J., (1991), “Comparison of existing methods for building triangular irregular network models of terrain from grid digital elevation models.”, *International Journal of Geographical Information Systems* 5 (3), 267–285.

Li, Z., Zhu,Q. and Gold,C., (2005). DigitalTerrain Modeling: Pronciples and Methodology. ISBN0-415-32462-9, 323 pp., CRC Press.

Lee, J.D., Han, S.H., Lee, S.S., Park, J.S., (2008), “Correcting DEM extracted from aster stereo images by combining cartographic DEM”. *The International Archives of the Photogrammetry, Remote Sensing and Spatial Information Sciences*. Vol. XXXVII. Part B8, pp 829-833

Lang, H.R. and Welch, R., (1999), “Algorithm Theoretical Basis Document for ASTER Digital Elevation Models, Version 3.0. Jet Propulsion Laboratory.”, Pasadena, California, USA , pp 1-63.

Maune, D.F., Kopp, S.M., Crawford, C.A., and Zervas, C.E., (2007). Digital Elevation

Models. "Digital Elevation Model Technologies and Applications: The DEM Users Manual." Ed. Maune, D.F. Bethesda, MD: *The American Society for Photogrammetry and Remote Sensing*. pp 1-6.

Miller L.M., (2011). "Analysis of Viewshed Accuracy with Variable Resolution LIDAR Digital Surface Models and Photogrammetrically- Derived Digital Elevation Models.", International Journal of Geographical Information Science, pp 4-34.

Mitášová, H., Hofierka, J., 1993. Interpolation by regularized spline with tension, II Application to terrainmodelling and surface geometry analysis. Mathematical Geology 25, 657–669.

Nelson, A., Reuter, H. I. and Gessler, P., (2009), " DEM production methods and sources". In: *Geomorphometry: concepts, software, applications.* T.Hengl & H. I. Reuter (eds.): pp 65–86. Developements in Soil Science, Vol. 33. Elsevier, Amsterdam.

Nikolakopoulos, K. G., Kamaratakis, E. K. and c, N. Chrysoulakis., (2006), "SRTM vs ASTER elevation products. Comparison for two regions in Crete, Greece". *International Journal of Remote Sensing*, 27, pp 4819–4838

Oksanen, Juha., (2006), "Digital Elevation Model error in terrain analysis." PhD-Thesis, Department of Geoinformatics and Cartography, Finnish Geodetic Institute. University pf Helsinki.Masala,Finland, 369 pp.

Peng, W., Petrovic, D., Crawford, C., (2004), "Handling Large Terrain Data in GIS.", *International Archives of Photogrammetry Remote Sensing and Spatial Information Sciences*. Vol 35; Part 4, pp 281-286.

Pike, R.J. Evans, I.S. and Hengl T., (2009) "Geomorphometry: A Brief Guide". In: *Geomorphometry: concepts, software, applications.* T.Hengl & H. I. Reuter (eds.): 8 pp. Developements in Soil Science, Vol. 33. Elsevier, Amsterdam.

Podobnikar T. (2005)., "Production of integrated digital terrain model from multiple datasets of different quality.", IJGIS, 19/ 1, 69–89. DOI : 10.1080/ 13658810412331280130

Sadick A.,Amfo-out R.,Acquah J. S., Nketia K. A., Asamoah E., Adjei O. E., (2015), "Assessment Of Heavy Contamination In Soils Around Auto Mechanic Workshop Clusters In Central Agricultural Station, Kumasi-Ghana", Applied Research Journal. 1(2), pp 12-19.

San, B.T. and Suzen, M.L., (2005)," Digital elevation (DEM) generation and accuracy assessment from ASTER stereo data.", *International Journal of Remote Sensing*, 26, pp 5013-5027

Shi, W.Z., Q.Q. Li, C.Q. Zhu, (2005), "Estimating the propagation error of DEM from higher-order interpolation algorithms." *International Journal of Remote Sensing*. Vol. 26, No. 4, pp:
3069-3084.

Smith, S.L., Holland, D.A., and Longley, P.A., (2004), "The Importance of Understanding Error in LiDAR Digital Elevation Models". *International Archives of the Photogrammetry, Remote Sensing and Spatial Information Sciences*. XXXV, pp 996- 1001.39.

Toutin, T., (2008), "ASTER DEMs for geomatic and geoscientific applica- tions: a review". *Int. J. Remote Sens*., 29(7), pp 1855–1875.

Toutin, Th. and Cheng, Ph., (2002), "Comparison of automated digital elevation model extraction results using along-track ASTER and across-track SPOT stereo images." Optical Engineering, 41, pp 2102–2106.

Tomaz Podobnikar Methods for visual quality assessment of a digital terrain model S.A.P.I.EN.S 2.2 | 2009 : Vol.2

Toutin, Th. and Cheng, Ph., (2001), "DEM generation with ASTER stereo data." *Earth Observation Magazine*, 10, pp 10–13.

Trisakti, B. and Carolita, I., (2005), "Comparison result of DEM generated from ASTER stereo data and SRTM". In: Proceedings of Map Asia, GIS Development, Aug. 22-25, Jakarta (CD-ROM).

Watson, D., (1992), Contouring: *A Guide to the Analysis and Display of Spatial Data*, Pergamon Press, London, 1992.

Welch, R., Jordan, T., Lang, H., Murakami, H., (1998),” ASTER as a source for topographic data in the late 1990’s”, *IEEE Transac- tions on Geoscience and Remote Sensing* 36 (4), pp 1282–1289.

Weibel R., Heller, M., (1999), “Digital terrain modelling”. In: Maguire, D.J., Goodchild, M.F., Rhind, D.W. (Eds.), Geographical Information Systems, vol. 1. Longman, Harlow. pp. 269-297.

Xion Ping, (2003),”*Digital Elevation Model Extracted from ASTER in Support of the Coal Fireand Environment Research Project, China*.” *ITC*. pp 1-92,

APPENDIX

Appendix 1: Accuracy Assessment of Generated DTM

Table 4.1: Accuracy assessment of generated DTM from ASTER

GCP ID	EASTING(m)	NORTHING(m)	GCPs(M)	ASTER	ΔZ(ASTER-TOPOGRAPHIC MAP)
			ELEVATION(m)		
1	657246.369	738833.369	274	259	-15
2	657281.699	738902.97	274	268	-6
3	657291.621	738873.982	275	266	-9
4	657348.11	738831.014	275	278	3
5	657411.319	738746.754	274	294	20
6	657253.806	739053.471	274	264	-10
7	657586.53	739254.063	273	282	9
8	658175.8	738779.502	259	269	10
9	657956.848	738535.606	259	260	1
10	657964.542	738448.828	237	249	12
11	657902.867	738323.72	258	250	-8
12	657885.599	738171.195	258	254	-4
13	657821.167	738065.738	261	256	-5
14	657891.966	738017.052	259	256	-3
15	657968.523	738064.908	249	249	0
16	658579.983	738036.835	263	257	-6
17	658600.658	737950.052	259	254	-5
18	658452.827	737949.557	237	241	4
19	658464.599	737887.393	258	246	-12
20	657586.398	739341.058	274	265	-9
21	671800.76	720963.748	381	380	-1
22	670780.003	721353.334	290	291	1
23	666950.902	722189.323	274	271	-3
24	666450.749	722526.355	259	289	30
25	666502.951	723460.382	259	273	14
26	666754.835	723547.628	274	283	9
27	675876.054	724939.012	427	414	-13
28	675500.411	725022.416	442	438	-4
29	675537.968	725134.282	442	443	1
30	675602.09	725130.158	457	452	-5
31	675692.657	725090.735	442	443	1
32	674517.565	723807.378	351	349	-2
33	673480.587	703296.461	686	675	-11
34	673366.067	703401.69	640	651	11
35	672457.274	701991.168	533	537	4
36	669467.152	699490.959	442	445	3
37	670432.084	697242.79	681	679	-2
38	671471.561	716677.733	300	300	0
39	671141.261	717673.263	320	325	5
40	671368.552	718101.201	198	209	11
			RMSE		±9.239

	MAE	±7.050

Appendix 2: Accuracy assessment of the four interpolating algorithms on various terrains.

Table 4.2: Accuracy assessment of the four interpolating algorithms on the Flat terrain (Edwenase-Kwadaso (Agricultural Station))

GCP ID	EASTING(m)	NORTHING(m)	SPOT HEIGHTS(m)	SPLINE(M)	ΔZ_{SPLINE}	NN(m)	ΔZ_{NN}	KRIGING(m)	$\Delta Z_{KRIGING}$	IDW(m)	ΔZ_{IDW}
1	649,034.16	736,246.94	259	248.291	-10.709	248.281	-10.719	248.698	-10.302	248.065	-10.935
2	649,378.51	736,344.66	259	247.802	-11.198	247.854	-11.146	246.526	-12.474	248.007	-10.993
3	646,718.67	736,268.36	274	283.399	9.399	283.541	9.541	282.456	8.456	283.154	9.154
4	648,567.92	741,465.10	290	276.231	-13.769	276.536	-13.464	282.433	-7.567	279.033	-10.967
5	648,356.89	737,439.40	274	273.013	-0.987	272.929	-1.071	271.182	-2.818	272.995	-1.005
6	648,186.70	741,514.75	274	270.568	-3.432	270.548	-3.452	262.221	-11.779	272.425	-1.575
7	647,928.75	741,532.29	259	269.965	10.965	270.412	11.412	268.323	9.323	269.931	10.931
8	646,920.13	737,402.79	259	232.371	-26.629	232.096	-26.904	229.353	-29.647	231.970	-27.030
9	644,535.55	737,403.48	259	231.394	-27.606	231.345	-27.655	232.307	-26.693	231.300	-27.700
10	647,470.28	737,714.41	259	253.532	-5.468	249.460	-9.540	230.757	-28.243	253.603	-5.397
11	648,589.21	741,477.98	290	287.540	-2.460	287.240	-2.760	283.053	-6.947	288.193	-1.807
12	648,652.61	741,478.24	290	294.197	4.197	295.229	5.229	293.154	3.154	295.050	5.050
13	649,431.00	736,406.75	259	246.661	-12.339	246.373	-12.627	246.793	-12.207	247.736	-11.264
14	647,813.33	741,504.69	259	279.823	20.823	279.869	20.869	277.574	18.574	279.874	20.874
15	648,536.30	737,471.52	274	264.755	-9.245	264.833	-9.167	265.079	-8.921	264.949	-9.051
16	648,106.47	737,481.06	274	267.327	-6.673	267.245	-6.755	265.271	-8.729	267.004	-6.996
17	648,439.89	737,492.16	274	275.520	1.520	275.310	1.310	270.882	-3.118	274.800	0.800
18	648,428.67	737,403.41	274	273.127	-0.873	272.563	-1.437	267.531	-6.469	272.850	-1.150
19	648,039.39	737,710.92	274	263.750	-10.250	263.347	-10.653	265.877	-8.123	263.172	-10.828
20	648,393.57	737,716.32	274	275.763	1.763	275.759	1.759	277.900	3.900	276.128	2.128
21	648,477.87	740,150.35	290	295.694	5.694	294.650	4.650	280.896	-9.104	295.866	5.866
22	648,452.11	740,188.34	290	273.580	-16.420	273.129	-16.871	270.758	-19.242	274.232	-15.768
23	648,361.92	741,153.03	290	299.106	9.106	299.034	9.034	291.734	1.734	299.070	9.070

25	648,701.27	741,505.88	290	299.503	9.503	299.769	9.769	294.800	4.800	299.911	9.911	
26	646,788.75	736,274.43	274	288.394	14.394	288.351	14.351	282.755	8.755	287.270	13.270	
27	649,067.56	736,354.07	259	254.398	-4.602	254.381	-4.619	254.075	-4.925	254.204	-4.796	
28	648,941.20	736,392.88	259	254.865	-4.135	254.550	-4.450	251.202	-7.798	254.928	-4.072	
29	648,677.87	741,486.58	290	298.179	8.179	297.431	7.431	294.288	4.288	297.802	7.802	
30	649,390.39	741,450.77	290	296.813	6.813	297.431	7.431	301.973	11.973	296.245	6.245	
31	646,018.98	736,224.68	259	265.763	6.763	265.330	6.330	250.467	-8.533	265.951	6.951	
32	646,082.31	736,244.14	259	260.333	1.333	258.286	-0.714	248.084	-10.916	260.000	1.000	
33	648,574.53	737,439.97	274	262.139	-11.861	262.081	-11.919	262.240	-11.760	262.105	-11.895	
34	648,784.24	737,442.96	274	259.061	-14.939	259.711	-14.289	257.858	-16.142	259.880	-14.120	
35	648,477.87	740,150.35	290	295.694	5.694	294.650	4.650	280.896	-9.104	295.866	5.866	
36	648,452.11	740,188.34	290	273.580	-16.420	273.129	-16.871	270.758	-19.242	274.232	-15.768	
37	644,923.06	736,553.71	259	263.206	4.206	263.208	4.208	258.505	-0.495	263.005	4.005	-1.807
38	648,271.87	737,434.48	274	270.319	-3.681	269.797	-4.203	266.478	-7.522	269.922	-4.078	±10.773
39	648,567.92	741,465.10	290	276.231	-13.769	276.536	-13.464	282.433	-7.567	279.033	-10.967	
40	648,589.21	741,477.98	290	287.540		287.240	-2.760	283.053	-6.947	288.193		
24	648,370.09	741,165.87	290	299.691	9.691	298.613	8.613	290.858	0.858	299.649	9.649	
					-2.460							
		RMSE			±11.035		±11.121		±12.108			
		MAE			±8.999		±9.102		±9.979		±8.714	

Table 4.3: Accuracy assessment of the four interpolating algorithms on the undulating terrain (KNUST campus)

GCP ID	EASTING (M)	NORTHING(M)	GPS POINTS(m)	SPLINE(M)	ΔZSPLINE	NN(M)	ΔZNN	KRIGING(M)	ΔZKRIGING	IDW(M)	ΔZIDW

1	660,915.44	738,677.67	259	255.507	-3.557	255.789	-3.211	261.003	2.004	255.047	-3.953
2	657,886.61	741,140.94	274	271.177	-2.827	271.133	-2.867	269.658	-4.342	271.000	-3.000
3	661,401.03	741,155.87	274	263.606	-10.150	264.153	-9.847	266.861	-7.139	264.038	-9.962
4	656,609.99	741,209.81	259	266.508	7.500	265.611	6.611	249.679	-9.321	265.669	6.669
5	661,146.23	738,596.30	274	266.108	-8.053	264.886	-9.114	263.467	-10.533	265.731	-8.269
6	657246.369	738833.369	274	246.492	-27.407	246.785	-27.215	248.427	-25.573	247.038	-26.962
7	657281.699	738902.97	274	254.112	-19.954	253.685	-20.315	249.128	-24.872	253.916	-20.084
8	657291.621	738873.982	275	252.710	-22.679	251.405	-23.595	249.139	-25.861	251.857	-23.143
9	657348.11	738831.014	275	249.619	-25.892	249.237	-25.763	249.210	-25.790	249.106	-25.894
10	657411.319	738746.754	274	249.250	-24.774	249.169	-24.831	249.762	-24.238	249.009	-24.991
11	657253.806	739053.471	274	249.288	-24.795	248.839	-25.161	244.459	-29.541	248.923	-25.077
12	657586.53	739254.063	273	268.953	-3.984	268.896	-4.104	261.445	-11.555	268.955	-4.045
13	658175.8	738779.502	259	257.397	-2.906	255.387	-3.613	250.719	-8.281	255.888	-3.112
14	657956.848	738535.606	259	247.496	-11.926	247.528	-11.472	252.314	-6.686	247.069	-11.931
15	657964.542	738448.828	237	249.994	11.259	250.226	13.226	252.772	15.772	249.715	12.715
16	657902.867	738323.72	258	256.888	-1.282	256.457	-1.543	253.882	-4.118	255.891	-2.109
17	657885.599	738171.195	258	261.927	3.962	261.917	3.917	255.123	-2.877	261.998	3.998
18	657821.167	738065.738	261	255.248	-5.459	255.528	-5.472	254.456	-6.544	254.236	-6.764
19	657891.966	738017.052	259	252.072	-6.918	252.532	-6.468	253.859	-5.141	252.031	-6.969
20	657968.523	738064.908	249	252.145	5.356	255.929	6.929	254.597	5.597	254.160	5.160
21	658579.983	738036.835	263	249.794	-13.961	251.604	-11.396	254.528	-8.472	253.013	-9.987
22	658600.658	737950.052	259	248.953	-9.502	251.257	-7.743	253.140	-5.860	253.470	-5.530
23	658452.827	737949.557	237	248.475	11.195	248.658	11.658	253.087	16.087	248.206	11.206
24	658464.599	737887.393	258	255.694	-2.504	255.103	-2.897	253.585	-4.415	254.844	-3.156
25	657586.398	739341.058	274	268.953	-7.905	268.896	-5.104	261.445	-12.555	268.955	-5.045
			RMSE		±13.717		±13.711		±14.835		±13.549
			MAE		±11.028		±10.963		±11.658		±10.789

Table 4.4: Accuracy assessment of the four interpolating algorithms on the mountainous terrain (Lake Bosomtwi and surrounding regions)

GCP ID	EASTING (M)	NORTHING(M)	SPOT HEIGHTS(m)	SPLINE(M)	ΔZ_{SPLINE}	NN(M)	ΔZ_{NN}	KRIGING(M)	$\Delta Z_{KRIGING}$	IDW(M)	ΔZ_{IDW}
1	671800.76	720963.748	381	368.913	-12.087	372.020	-8.980	349.927	-31.073	371.646	-9.354
2	666450.749	722526.355	274	277.789	3.789	291.189	17.189	293.110	19.110	285.137	11.137

3	666754.835	723547.628	274	278.605	4.605	291.873	17.873	279.226	5.226	279.610	5.610
4	675537.968	725134.282	442	428.909	-13.091	443.813	1.813	409.582	-32.418	446.299	4.299
5	675692.657	725090.735	442	430.720	-11.280	458.451	16.451	415.993	-26.007	442.737	0.737
6	674517.565	723807.378	351	346.284	-4.716	320.100	-30.900	349.953	-1.047	343.108	-7.892
7	673480.587	703296.461	686	681.368	-4.632	681.141	-4.859	653.794	-32.206	669.899	-16.101
8	673366.067	703401.69	640	640.520	0.520	663.052	23.052	643.355	3.355	647.087	7.087
9	672457.274	701991.168	533	531.804	-1.196	533.015	0.015	527.574	-5.426	526.202	-6.798
10	669467.152	699490.959	442	464.151	22.151	423.224	-18.776	447.070	5.070	430.890	-11.110
11	673259.37	699120.2	442	443.877	1.877	497.297	55.297	480.943	38.943	444.118	2.118
12	672803.87	698735.18	640	649.123	9.123	640.248	0.248	630.767	-9.233	649.409	9.409
13	673886.95	704989.07	427	420.723	-6.277	401.488	-25.512	451.801	24.801	421.065	-5.935
14	670017.87	700071.84	396	399.614	3.614	397.311	1.311	393.997	-2.003	399.580	3.580
15	672094.17	701184.97	533	457.202	-75.798	514.933	-18.067	514.073	-18.927	457.346	-75.654
16	671628.49	700562	549	569.667	20.667	555.385	6.385	561.913	12.913	570.018	21.018
17	667072.28	718708.67	305	307.141	2.141	299.247	-5.753	305.983	0.983	306.851	1.851
18	680672.71	718700.95	259	240.537	-18.463	257.569	-1.431	262.853	3.853	236.143	-22.857
19	684873.88	720522.03	259	246.207	-12.793	251.110	-7.890	249.007	-9.993	246.261	-12.739
20	668181.29	721348.51	290	295.966	5.966	294.924	4.924	288.011	-1.989	295.972	5.972
21	676,820.49	711,071.01	530	502.699	-27.301	526.734	-3.266	500.720	-29.280	501.822	-28.178
22	674,767.72	714,872.29	294	302.423	8.423	310.982	16.982	311.886	17.886	302.673	8.673
23	671,792.68	710,192.91	290	288.932	-1.068	295.869	5.869	281.030	-8.970	288.963	-1.037
24	675,321.91	711,493.09	393	430.110	37.110	405.443	12.443	399.931	6.931	429.078	36.078
25	681,601.38	710,144.34	533	545.420	12.420	492.261	-40.739	537.966	4.966	545.538	12.538
26	670,715.84	710,692.65	290	298.627	8.627	298.786	8.786	286.034	-3.966	298.468	8.468
27	678,545.59	711,174.04	564	557.320	-6.680	574.518	10.518	613.819	49.819	556.729	-7.271
28	676,861.42	711,017.71	534	543.514	9.514	530.081	-3.919	522.950	-11.050	543.499	9.499
29	674,628.20	711,681.06	393	395.061	2.061	368.812	-24.188	394.604	1.604	395.235	2.235
30	671,320.06	711,882.59	305	305.978	0.978	308.450	3.450	301.017	-3.983	305.943	0.943
31	676,323.54	711,568.33	488	489.079	1.079	472.028	-15.972	531.849	43.849	488.956	0.956
32	679,200.86	711,667.77	456	410.270	-45.730	453.258	-2.742	455.879	-0.121	410.607	-45.393

33	674,176.21	709,329.47	503	481.716	-21.284	485.337	-17.663	492.015	-10.985	481.932	-21.068
34	669,195.18	710,822.66	274	281.043	7.043	286.313	12.313	276.013	2.013	281.019	7.019
35	677,737.19	711,274.23	549	557.913	8.913	573.558	24.558	609.522	60.522	557.627	8.627
36	675,659.65	712,061.90	366	412.425	46.425	387.064	21.064	378.994	12.994	412.422	46.422
37	675,864.94	711,743.83	413	449.358	36.358	418.822	5.822	421.102	8.102	448.601	35.601
38	683,966.26	715,737.93	443	397.740	-45.260	391.107	-51.893	421.006	-21.994	397.837	-45.163
39	675,710.04	712,434.05	362	348.445	-13.555	358.313	-3.687	340.947	-21.053	348.119	-13.881
40	667,711.41	712,469.08	271	263.848	-7.152	267.256	-3.744	266.017	-4.983	263.846	-7.154
			RMSE		±21.721		±19.044		±21.167		±21.632
			MAE		±14.544		±13.909		±15.241		±14.687